ACCSCIENCE PUBLISHING

Asian Journal of Water, Environment and Pollution

ORIGINAL RESEARCH ARTICLE

Big data-driven carbon footprint tracking and game-theoretic incentive design in green logistics supply chains

Lin Sun[1]*, and Jun Zeng[2]

[1]School of Accounting and Finance, Shandong Vocational and Technical University of International Studies, Rizhao, Shandong, China

[2]Research Office, Shandong Vocational and Technical University of International Studies, Rizhao, Shandong, China

(This article belongs to the *Special Issue: Pathways to Carbon Neutrality and Low-Carbon Energy Transition in China: Policy, Technology, and Systemic Innovation*)

Abstract

This study examines big data-driven carbon footprint tracking in green supply chains and the design of game-theoretic incentive mechanisms, with a focus on China's logistics industry. We develop a comprehensive analytical framework integrating machine learning prediction, network topology analysis, and multi-agent evolutionary game theory. Using road freight statistics and operational data from 2018 to 2023, we model and forecast logistics carbon emission intensity through multiple regression and machine learning models. Complex network metrics were applied to characterize the interregional carbon emission correlation structures and identify high-emission nodes. Building on this, the study introduces three key actors—government regulators, logistics enterprises, and suppliers—and establishes functions for emission reduction subsidies and excess emission penalties. An evolutionary game model is formulated, and numerical simulations examine how subsidy intensity and penalty severity influence the system's evolutionary equilibrium. Results indicate that China's logistics carbon emissions exhibit a temporal pattern of initial growth followed by stabilization. Spatially, emissions cluster prominently in transportation- and industry-dense regions such as North China, the Yangtze River Delta, and the Pearl River Delta, with high-emission nodes exhibiting high centrality within the network. When incentive parameters are weak, enterprises tend to adopt passive emission reduction strategies. However, under scenarios with higher subsidies and moderate penalties, the proportion of enterprises adopting emission reduction strategies increases in an S-shaped manner over time, ultimately converging to a low-carbon stable equilibrium. The findings indicate that combining big data-driven carbon footprint tracking with differentiated subsidy–penalty policies helps identify regional priority emission reduction targets and critical links, providing quantitative support for designing collaborative emission reduction policies and incentive mechanisms tailored to logistics supply chains.

Keywords: Green supply chain; Carbon footprint; Logistics industry; Big data analysis; Evolutionary game theory

***Corresponding author:**
Lin Sun
(linsun2021@163.com)

Citation: Sun L, Zeng J. Big data-driven carbon footprint tracking and game-theoretic incentive design in green logistics supply chains. *Asian J Water Environ Pollut.* 2026;23(3):026040017.
doi: 10.36922/AJWEP026040017

Received: January 23, 2026

Revised: March 7, 2026

Accepted: March 12, 2026

Published online: April 29, 2026

1. Introduction

The global logistics and transportation sector accounts for approximately 8% of worldwide greenhouse gas emissions.[1] With China's "dual carbon" goals, the logistics industry faces increasing pressure for energy conservation and emission reduction.[2] In recent years, China's freight activity has continued to expand, while transport remains a major energy-consuming end-use sector, accounting for 16% of total final energy consumption in 2023.[3] Policy releases from China's transport authorities report that as of the end of 2020, more than 430,000 new-energy urban logistics distribution vehicles were operating nationwide, supported by green urban freight distribution pilots and demonstration programs.[4] In parallel, leading logistics platforms (e.g., JD Logistics) have accelerated fleet electrification by adopting electric delivery vehicles and supporting charging infrastructure. However, China's logistics sector remains largely fragmented, with significant information asymmetry hindering the adoption of low-carbon technologies. Establishing an efficient carbon emissions monitoring and incentive mechanism is crucial for advancing the green transformation of logistics and achieving carbon peaking.

Existing research has explored logistics decarbonization from multiple angles, including green supply chain coordination, carbon monitoring, big data and machine learning (ML), incentive policies, and evolutionary game models. However, the existing literature still leaves three concrete gaps. First, carbon monitoring studies often focus either on macro inventories or firm-level accounting, while the cross-regional linkage structure of logistics emissions and its implications for targeted interventions remain underexplored. This study addresses this by constructing a cross-regional logistics-carbon emission linkage network (macro indicators integrated with transportation management system [TMS]/on-board diagnostics [OBD]/global positioning system [GPS] microdata) and diagnosing high-impact nodes using centrality and linkage-strength metrics. Second, ML-based emission prediction is often developed as a standalone tool and is rarely coupled with policy-incentive design, making it difficult to translate predictive insights into actionable subsidy/penalty rules. To bridge this measurement-to-policy gap, this study embeds ML-predicted emission baselines into the game incentives and derives implementable threshold ranges for subsidy and penalty. Third, evolutionary game studies typically adopt stylized payoff settings that do not incorporate data-informed emission baselines or network-derived heterogeneity, and the joint responses of strategies to subsidy and penalty parameters are rarely mapped systematically. This study further parameterizes heterogeneous payoffs with data-informed emissions and network-derived roles, and maps strategy dynamics over the subsidy–penalty policy space via response surface analysis.

To address these gaps, this study makes three ranked contributions. First, as the core contribution, it proposes a data-informed integrated framework that links big data-driven carbon emission prediction and logistics-carbon emission linkage network diagnostics with a multi-agent evolutionary game, enabling the derivation of threshold ranges for subsidy and penalty policies. Second, it constructs a logistics–carbon emission linkage network and identifies key emission nodes for differentiated governance based on network metrics. Third, it provides a response surface analysis of policy parameters and translates simulation outcomes into targeted recommendations for enterprises and regulators.

2. Literature review

2.1. Decarbonizing logistics and supply chains: Scope 3, digital transformation, and policy instruments

Early green supply chain research established that carbon constraints and coordination incentives must be modeled jointly: foundational game-theoretic coordination mechanisms explicitly embedding emissions management provide the baseline for subsequent incentive designs.[5] Recent studies have shifted from firm-internal (Scopes 1–2) accounting toward value-chain (Scope 3) measurement, verification, and financial materiality. Empirical evidence shows that validated Scope 3 disclosures can influence firm valuation, strengthening the business case for credible measurement, reporting, and verification (MRV) in manufacturing supply chains.[6] In parallel, the post-pandemic period has elevated resilience as a co-equal objective with sustainability, motivating integrated frameworks for sustainable and resilient logistics operations.[7] Systematic reviews further synthesize the rapidly expanding Scope 3 and green supply chain literature, clarifying dominant approaches and persistent empirical gaps.[8]

At the operational level, supplier-oriented mitigation strategies and buyer–supplier governance are increasingly analyzed as interdependent capability portfolios rather than isolated practices.[9] Methodological agenda pieces emphasize moving beyond "counting emissions" toward impact pathways that connect data, incentives, and outcomes along the chain.[10] Recent network design work highlights multimodal logistics as a practical approach to complying with carbon caps while maintaining service levels, particularly when modal substitution and routing

are jointly optimized.[11] Complementing these operations-focused strands, data-driven digital transformation is repeatedly identified as the enabling layer for carbon neutrality—linking sensing, data integration, and decision analytics across tiers.[12]

A central policy question is how different carbon pricing regimes propagate through supply chain decisions. Comparative analyses of carbon tax versus cap-and-trade regimes show that the choice of instrument changes equilibrium production, ordering, and abatement incentives, and thus should be explicitly modeled in mechanism design.[13] Blockchain-enabled traceability and verification have been studied to reduce information asymmetry in Scope 3 disclosure and to improve the credibility of reporting to downstream stakeholders.[14] On the logistics side, low-carbon fourth-party logistics network design under cap-and-trade demonstrates how centralized coordinators can internalize carbon prices in routing and facility decisions.[15] In the face of demand and yield uncertainty, robust and stochastic formulations help clarify when green manufacturing investments remain cost-effective.[16]

Recent optimization research on sustainable supply chains under trade credit and carbon constraints shows that inventory decisions, financing conditions, and emissions limits must be jointly modeled to identify cost-effective low-carbon operating policies.[17] Beyond domestic pricing, carbon border adjustment measures and tariffs reshape sourcing and logistics strategies; recent evidence and modeling work document strategic coping responses and potential unintended consequences along international supply chains.[18] Recent discussions of sustainable supply chain practices further summarize operational and managerial levers for Scope 3 mitigation.[19] Recent operations management research highlights that the management of greenhouse gas emissions in supply chains is shaped by systemic sources of uncertainty, implying that Scope 3 reduction strategies must be supported by stronger governance, coordination, and information-sharing mechanisms across multi-tier supplier networks.[20] Quantitative optimization studies further detail how emissions can be reduced in multi-echelon production–distribution systems and how mixed-integer programming and matheuristics scale to real-world problem sizes.[21,22] However, empirical auditing of logistics emissions reporting suggests persistent data-quality limitations—especially in fragmented logistics markets—implying that purely data-intensive approaches may fail without MRV governance.[23] Recent empirical evidence suggests that supply chain resilience can be significantly strengthened through effective resource orchestration, especially through internal resource reconfiguration and external integration, while artificial intelligence assimilation further amplifies the positive effects of these strategies on readiness and recovery capabilities.[24]

2.2. Emissions estimation and forecasting: From black-box prediction to leakage-free explainability

Comprehensive benchmarking on structured data for both regression and classification shows that no single model dominates across all task settings, but well-tuned ML baselines remain highly competitive, providing an empirical basis for careful model comparison and for retaining gradient-boosted decision trees (GBDT; e.g., light gradient boosting machine [LightGBM]) as strong candidates in logistics emissions prediction tasks.[25] In parallel, recent studies on low-carbon logistics-carbon emission linkage network planning under uncertain demand show that carbon-efficient freight configuration requires the joint optimization of transport structure, routing, and regional network layout,[26] while research on sustainable and resilient intermodal transport networks further demonstrates that disruption management must be integrated with sustainability objectives when designing robust logistics systems.[27]

High prediction accuracy alone is insufficient for policy and managerial adoption; explainability is increasingly treated as a first-class requirement. Shapley-based explainability methods tailored to time-series artificial intelligence models show that preserving temporal structure is essential for producing coherent and actionable explanations in sequential prediction tasks,[28] while Window Shapley additive explanation (SHAP) proposes an efficient window-based explanation strategy for time-series classifiers.[29] These tools enable attribution of emissions to drivers, such as congestion, payload ratio, speed profile, and routing—provided that model training and evaluation are designed to avoid temporal leakage.

Recent applications of ML for transport emissions estimation provide empirical templates and feature engineering choices for logistics settings.[30] Related transportation sensing studies (e.g., autonomous monitoring) further demonstrate how high-frequency data streams can support more granular emission metering and enforcement.[31] Classical time-series baselines remain relevant: improved autoregressive integrated moving average variants can yield competitive short-horizon forecasts for aggregate emissions when data are stable and stationary assumptions approximately hold.[32] In spatially heterogeneous environments, multi-scale characterization frameworks that combine land-use information with interpretable ML demonstrate how domain structure can

be incorporated while retaining explainability.[33]

Domain-specific explainable ML studies on vehicle carbon dioxide (CO_2) emissions underscore the practical value of transparent feature attributions for engineering and policy decisions,[34] and country-level analyses further show how model performance and drivers differ across geographies and fleet compositions.[35] Open and reproducible benchmarking studies of daily CO_2 forecasting models emphasize rigorous evaluation protocols, transparent code and data availability, and systematic comparisons across statistical, ML, deep learning, and hybrid approaches.[36] Explainable ML studies on transport-related CO_2 emissions indicate that combining predictive accuracy with transparent feature attribution can improve model credibility and policy relevance, especially when emissions are jointly shaped by physical operating conditions and managerial decisions.[37]

Explainable forecasting studies in transport and energy emissions contexts show that interpretable models can reveal key and time-varying drivers of system performance and emissions, thereby improving the policy relevance and managerial usability of prediction results.[38,39] In addition, sector-specific forecasting studies show that demand-side variation can be explicitly linked to downstream energy consumption and CO_2 emissions, providing transferable insights into activity-to-emission mapping, temporal uncertainty, and model selection for applications.[40] Deep learning architectures such as convolutional long short-term memory have been explored for forecasting freight demand, a key upstream driver of logistics emissions forecasting pipelines.[41] Road freight forecasting studies further demonstrate that freight flow projections can be translated into greenhouse gas emission estimates for sustainable transportation planning, reinforcing the value of integrating activity forecasting with emissions accounting.[42] Finally, transportation system control studies show that operational policies (e.g., right-of-way allocation) can meaningfully change emissions outcomes, motivating an integrated "predict–optimize–incentivize" framing.[43] In regional empirical contexts, ML-based emission prediction and driver analysis demonstrate the feasibility of high-resolution forecasting linked to policy levers.[44]

2.3. Incentive mechanism design: Evolutionary and dynamic games for low-carbon collaboration

Given that low-carbon logistics requires coordinated actions across government, platform operators, carriers, shippers, and consumers, game-theoretic models—particularly evolutionary games—are widely used to capture bounded rationality, learning, and policy adaptation. Recent evolutionary game models analyze emissions reduction in complex supply chains and characterize how subsidies, penalties, and information disclosure shift strategy adoption over time.[45] Complementary work examines interactions between governments and enterprises under carbon reduction policies, clarifying when regulation induces stable low-carbon equilibria.[46] At the logistics cluster level, evolutionary game studies on green packaging diffusion show that peer effects, regulatory intensity, and financial support jointly shape the speed and stability of low-carbon practice adoption.[47]

In maritime contexts, tripartite evolutionary games incorporate shipper–carrier–port (or regulator) interactions and show how collaboration can be sustained when carbon pricing and cooperative benefits are jointly considered.[48] In cold chain logistics, evolutionary game theory shows that environmental regulation and green credit jointly shape the adoption of low-carbon operations, and that financing conditions can materially affect the speed and stability of strategic convergence.[49] Consumer behavior is also central: evolutionary game formulations linking manufacturers and consumers demonstrate how green preferences and information affect equilibrium strategies and welfare outcomes.[50] Multi-agent evolutionary games provide more general frameworks to capture heterogeneous agents and multiple competing strategies in low-carbon manufacturing and logistics environments.[51]

Evolutionary game frameworks have also been applied directly to logistics platforms and freight transport coordination problems, showing how incentives for capacity sharing, information exchange, and service provision influence cooperative stability among carriers, shippers, and platforms.[52] Logistics-related studies on fresh e-commerce and cold chain collaboration further show how incentive mechanisms and supervision policies shape cooperative stability and low-carbon governance outcomes.[53] More recent logistics-focused analyses extend this line of work to tripartite interactions among governments, logistics enterprises, and consumers under the "dual carbon" agenda, highlighting how policy intensity and infrastructure support can accelerate convergence toward low-carbon equilibria.[54] Cap-and-trade-based cooperative emission reduction behavior has also been explored, underscoring the importance of allowance allocation rules and coordination mechanisms.[55]

Blockchain and data-sharing technologies introduce a new strategic layer by altering information asymmetry, traceability, and the feasibility of enforcement. Evolutionary game analysis of blockchain traceability adoption in low-carbon supply chains provides a direct basis for modeling traceability-driven compliance in carbon accounting

systems.[56] Related studies examine government–enterprise interactions under environmental supervision[57] and the evolutionary dynamics of low-carbon logistics strategies in two-level supply chains under a carbon tax policy.[58] In logistics-specific settings, blockchain-enabled incentive mechanisms for information sharing in port cold chain networks further illustrate how smart contract-style rewards and verification can sustain cooperation and reduce opportunistic behavior.[59]

Additional evolutionary analyses in blockchain-enabled regional logistics-carbon emission linkage network and maritime logistics alliances further show that participation incentives, benefit-distribution rules, and network structure critically determine whether cooperative information-sharing and low-carbon strategies become stable over time.[60,61] Dynamic game models beyond evolutionary settings, such as sequential games in emissions trading schemes, formalize intertemporal strategic behavior under trading rules.[62] Policy support modeling for carbon capture and storage shows how market perceptions and policy credibility affect investment equilibrium.[63] Finally, game-theoretic evolution in renewable energy systems highlights how technological transitions can be modeled as co-evolving strategies among multiple stakeholders.[64]

2.4. Network-based carbon transfer analysis: From spatial interactions to key node identification

Spatial equilibrium models of regional emission regulation quantify how policy shocks propagate across sectors and provinces through regional–sectoral linkages, providing a macro-level basis for understanding how local interventions generate non-local carbon spillovers.[65] In transport-specific settings, assessments of CO_2 ship transport systems show that technical and economic constraints shape viable decarbonization pathways for long-distance trade.[66] At the regional development level, studies on the decoupling of carbon emissions and economic development document heterogeneous trajectories across cities and indicate that differentiated low-carbon transition policies are needed to reflect regional differences in energy and industrial structure.[67]

Spatiotemporal analyses of urban traffic carbon emissions and their drivers support more granular transport network construction and help identify where carbon-intensive corridors and regional hotspots are likely to concentrate.[68] Spatial network studies further reveal how interregional interactions and industrial linkages shape the topology of carbon-intensity networks.[69] The construction and characterization of urban correlation networks provide empirical tools for identifying structural features (e.g., core–periphery) and key transmission pathways in city-level carbon systems.[70] In multimodal transport networks, carbon price scenarios can induce structural transitions, reinforcing the value of network-aware policy analysis.[71]

Methodologically, complex network analysis has been applied to carbon emission transfers under global value chains, revealing community structures and high-impact transfer relationships that help identify dominant nodes and edges in logistics-carbon emission linkage network.[72] Industry-level identification of key carbon emission sectors demonstrates how network and ranking methods can prioritize mitigation targets.[73] Efficient computation of Katz centrality enables scalable estimation of global influence metrics on large networks, which is essential when logistics networks contain millions of shipments or nodes.[74] Collective influence maximization and optimal percolation research further provide algorithmic foundations for finding "influencers" in spreading processes, offering a principled way to locate key nodes in carbon spillover networks.[75-77]

Finance and policy interactions also have network implications: empirical evidence links green finance to lower carbon intensity, suggesting that financial resource allocation can reshape emissions networks via investment and technology diffusion.[78] Low-carbon pilot city policies and corporate financialization have been associated with measurable changes in environmental outcomes, implying that policy experiments can induce structural shifts in carbon-related networks over time.[79] Beyond simple graphs, hypergraph-based methods for locating influential nodes capture higher-order interactions (e.g., multi-party contracts or hub-and-spoke shipment bundles) that are common in logistics ecosystems.[80]

Recent network-based evolutionary game research on corporate carbon information disclosure shows that incentive and constraint mechanisms can reshape disclosure behavior across market contexts, highlighting how information propagation and regulatory pressure jointly affect the credibility of carbon disclosure systems.[81] Methodological studies on PageRank centrality for weighted and directed networks clarify the assumptions embedded in ranking metrics and provide a rigorous basis for metric selection in directed carbon flow networks.[82] Broader reviews of centrality measures in transportation networks further support the practical use of centrality-based diagnostics to identify critical nodes and vulnerable corridors in climate-related transport planning.[83] Finally, extensions of PageRank-like centrality to multiplex networks motivate multi-layer modeling when physical, information, and financial flows jointly determine carbon

outcomes.[84]

2.5. Synthesis, structured comparison, and research positioning

Across these strands, three consistent gaps emerge: (i) emissions estimation is often separated from incentive design, leaving a disconnect between "measurement" and "behavioral change"; (ii) network externalities and spillovers are frequently acknowledged but rarely embedded into the game mechanisms that govern multi-actor cooperation; and (iii) explainability is sometimes treated as a post-hoc visualization rather than a leakage-free, decision-relevant diagnostic. Accordingly, the present study positions itself at the intersection of (i) data-driven carbon footprint tracking and prediction, (ii) topology-aware identification of high-impact nodes/paths, and (iii) game-theoretic incentive mechanisms that internalize both carbon costs and information asymmetry (Table 1).

3. Methodology

The methodological design comprises two components: big data-driven carbon emission forecasting and network analysis, along with the construction of a supply chain evolutionary game model.

3.1. Big data emissions forecasting and network topology analysis

Based on logistics industry statistics and operational data, a carbon emissions forecasting model was first established. Multivariate regression and ML algorithms were employed to screen and model factors influencing carbon emissions, including transport distance, vehicle speed, load, vehicle type, and fuel type. Lasso regression or principal component analysis was used to extract key influencing factors, reducing multicollinearity and compressing dimensions. All preprocessing steps were implemented in Python, with numeric feature scaling conducted using StandardScaler from scikit-learn (version 1.8.0).

The modeling phase incorporated time-series cross-validation and stratified leave-one-out validation, comparing LightGBM, support vector regression (SVR), and Prophet, along with their "exogenous variable" extensions. Evaluation metrics included root mean square error (RMSE), mean absolute percentage error (MAPE), and weighted MAPE, with residuals tested for white noise and autocorrelation. To enhance interpretability, SHAP and partial dependency analysis were used to characterize the marginal effects of key factors, while quantile regression or bootstrapping provided prediction intervals to quantify uncertainty. Separate models were built for different business lines—trunk routes, branch routes, same-city routes, cold chain, express freight, and courier services—and for energy types—diesel, gas, pure electric, and hybrid. These were then integrated via stacking generalization to form global forecasts, ensuring robustness under structural differences.

Subsequently, a topological analysis was conducted on the logistics-carbon emission linkage network. This study constructed a directed network at the regional (province/city) level, where nodes represent regions (or aggregated enterprise clusters) and edges represent carbon flows along origin–destination (OD) logistics corridors. Specifically, for each shipment/order n departing from origin i to destination j within a time window t, shipment-level carbon emissions were computed as **Equation 1**:

$$C_{n,ijt} = q_n d_n e^n \tag{1}$$

where is q_n freight quantity (t), d_n is transport distance (km), and e^n (kg CO_2 per ton km) is the predicted carbon emission intensity output by the ML model using operational features (e.g., speed, load factor, vehicle type, and fuel/energy). The edge weight (carbon emission linkage strength) was then operationally defined as the aggregated carbon flow. This study aggregated shipment records into annual networks for 2018–2023 (and a pooled network for robustness), retaining directionality. For cross-year comparability, this study reports both the raw weighted network and a normalized network with row normalization (required for transition-based measures such as PageRank). This study further conducted sensitivity checks using global share normalization and edge-thresholding (e.g., removing the bottom 5% of weights) to reduce noise from sporadic low-volume links. Figure 1 reports the resulting region–corridor carbon-intensity matrix, where darker yellow cells indicate high-carbon "region–corridor" pairs, whereas blue-green cells correspond to low-carbon segments.

In multi-leg shipments and edge-weight allocation, some shipments traversed intermediate hubs (e.g., Chengdu→Wuhan→Shanghai). When leg-level route information was available from the transport management system or waypoint logs, this study decomposed each shipment into ordered legs and allocated predicted emissions to each leg in proportion to the leg's transport work. Accordingly, each directed edge (i→j) aggregated the carbon flow on the corresponding transport leg, and the edge weight $w\_\{ij,t\}$ was defined as the sum of leg-level predicted emissions within time window t. For records in which only the OD pair was observed and intermediate stops were unavailable, emissions were aggregated to the OD edge and treated as an OD-only approximation. To

Table 1. Structured comparison of representative studies and how they inform the present study

Theme/focus	Reference(s)	Data/context	Method	Key finding	Implication for this study
Carbon-aware supply chain coordination	Huang *et al.*[5]	Generic supply chain	Game-theoretic coordination	Jointly modeling incentives and emissions constraints is necessary	Mechanism design must internalize both cost and carbon
Scope 3 MRV & governance under uncertainty	Tian *et al.*;[6] Harju *et al.*[20]	Manufacturing/ supply chain greenhouse gas management	Empirical finance + operations-management analysis	Verified Scope 3 information is financially material, while emissions management is strongly shaped by systemic uncertainty and governance capability	Traceable MRV and uncertainty-aware coordination are prerequisites for scalable incentives
Resilient & sustainable logistics	Pan *et al.*;[7] Hasani Goodarzi *et al.*[27]	Global logistics/ intermodal transport network	Conceptual + network optimization	Sustainability and resilience should be jointly evaluated in intermodal logistics systems under disruption	Incentives should remain robust under shocks and network reconfiguration
Digital transformation for neutrality	Belhadi *et al.*;[12] Chen *et al.*[14]	Supply chain digitization/ blockchain	Data-driven transformation + traceability	Digital integration reduces information frictions in Scope 3 disclosure	Data infrastructure is an enabling layer for carbon tracking
Policy instrument comparison	Hua *et al.*;[13] Zhou *et al.*[18]	Carbon pricing/ tariffs	Analytical + quantitative models	Instrument choice changes equilibrium decisions and mitigation intensity	The model should explicitly represent carbon policy regimes
Structured-data prediction benchmark	Shmuel *et al.*[25]	Structured datasets for regression and classification	Benchmarking machine learning vs deep learning	Model performance varies across structured-data tasks, so systematic benchmarking is needed before selecting a predictive architecture	Supports careful comparison of GBDT/ LightGBM against alternative ML and DL models in logistics emissions prediction
Leakage-free explainability	Franco de la Peña *et al.*;[28] Nayebi *et al.*[29]	Time-series modeling	TimeSHAP / WindowSHAP	Explanations must respect temporal structure to be decision-relevant	Adopt a leakage-free pipeline + time-aware SHAP explanations
Transport emissions ML applications	Li *et al.*;[30] Yuan *et al.*[34]	Transport/vehicle emissions	ML estimation + XAI	Predictive accuracy improves with heterogeneous features; XAI aids actionability	Feature attribution guides which operational levers to incentivize
Network influence metrics	Noferini & Wood;[74] Morone & Makse[76]	Large networks / spreading processes	Katz centrality + optimal percolation	Global influence can be computed efficiently and identifies key spreaders	Use global centralities/ collective influence to locate high-impact nodes/ paths in carbon networks
Multi-layer network perspective	Zhang *et al.*;[80] Agryzkov *et al.*[84]	Multiplex/ hypergraph networks	Multiplex PageRank + hypergraph centrality	Higher-order and multi-layer interactions change node importance	Model physical, information, and financial layers jointly when possible

Abbreviations: DL: Deep learning; GBDT: Gradient-boosted decision trees; GBM: Gradient boosting machine; ML: Machine learning; MRV: Measurement, reporting, and verification; SHAP: Shapley additive explanations; XAI: Explainable artificial intelligence.

avoid double-counting, each shipment was recorded either as a decomposed leg sequence or as one aggregated OD edge, but never both simultaneously. Under this treatment, intermediate hubs received carbon flows only when they were explicitly observed in shipment trajectories, rather than being mechanically inferred from OD pairs.

To avoid any potential circularity in the estimation framework, the emission factor $\hat{e}_{f,n}$ used in the network construction was not treated as a self-generated quantity from the downstream game model or the network topology itself. Instead, the supervised-learning target was defined from ground-truth shipment-level carbon emission intensity derived from micro-level activity data. Specifically, for each shipment *n*, the label was constructed from observed fuel and/or electricity consumption records, converted into CO_2-equivalent emissions using calibrated accounting coefficients from authoritative emission factor inventories, and then normalized by transport work to obtain the emission intensity. Formally, the ground-truth emission intensity was defined as **Equation 2**:

$$e_{f,n} = C_n / (q_n d_n) \quad (2)$$

where C_n denotes total CO_2-equivalent emissions generated by shipment *n*, q_n is shipment volume, and d_n is the transport distance. When direct energy use records were available, C_n was calculated from observed fuel or electricity consumption multiplied by the corresponding conversion factors; when such records were incomplete, only shipments with verifiable activity-based accounting information were retained for supervised training. The ML model was then trained to predict this empirically constructed label rather than to generate the label itself. The resulting out-of-time predictions were subsequently used to parameterize network edge weights and game payoffs, while the label construction remained fully exogenous to the network and game modules.

Degree centrality, betweenness centrality, and clustering coefficient, respectively, measured a node's connectivity breadth, bridging role, and neighbor clustering within the network. Higher degree centrality indicates that a node maintains carbon emission links with more partners and occupies a more central position. Betweenness centrality reflects a node's intermediary role along multiple carbon flow paths, indicating its control over interregional carbon transmission. The clustering coefficient measures how tightly a node's neighbors are connected, revealing local carbon emission communities. To avoid bias from a single centrality family, this study further computed representative measures that capture distinct notions of node importance, including eigenvector centrality (influence through influential neighbors), Katz centrality (attenuated reachability), PageRank (random walk stationary importance on the directed, normalized network), and collective influence (influence-based identification of key spreaders). This study reports concordance/discordance across centrality families using rank correlations (Spearman) and top *k* overlap metrics (e.g., Jaccard), thereby quantifying the robustness of "key emission nodes" identification.

As shown in Figure 2, the logistics carbon emissions intensity heatmap illustrates the geographical distribution characteristics of carbon emissions in the logistics sector. The map reveals that high-emission areas are predominantly concentrated in the industrially developed eastern coastal regions and near inland transportation hubs, consistent with the aforementioned network analysis results and relevant research conclusions. Red "hotspot" areas represent higher carbon emission intensity per unit area or within specific regions, indicating that these zones concentrate substantial transportation activities and high-emission industries, making them priority targets for carbon reduction. Conversely, blue-green "coldspot" areas indicate lower carbon emission intensity. The national or regional logistics carbon emission intensity heatmaps generated by the actual model can further quantify regional emission disparities, clearly identifying hotspots and cold spots through spatial visualization. This enables policymakers to formulate differentiated reduction strategies: intensifying the adoption of clean transportation technologies and industrial restructuring in hotspot areas, while consolidating existing achievements and preventing emission rebounds in coldspot regions. In summary, integrating logistics-carbon emission linkage network topology analysis with spatial heat distribution maps effectively identifies high-emission hub cities and critical links, providing robust support for precise, science-based carbon reduction strategies.

3.2. Multi-agent evolutionary game model

To translate the data-driven emission insights into actionable policy design, this study formulated a tripartite evolutionary game among the government regulator, a focal logistics/manufacturing enterprise, and its upstream supplier. All agents were boundedly rational and updated strategies through imitation learning over time. The government chose strict regulation (R) or lenient regulation (L) with probability *x*; the enterprise chose proactive abatement (A_E) or passive/non-abatement (N_E) with probability *y*; and the supplier chose proactive abatement (A_S) or passive/non-abatement (N_S) with probability *z*. Baseline emissions and abatement potentials were grounded in the shipment-level carbon estimates

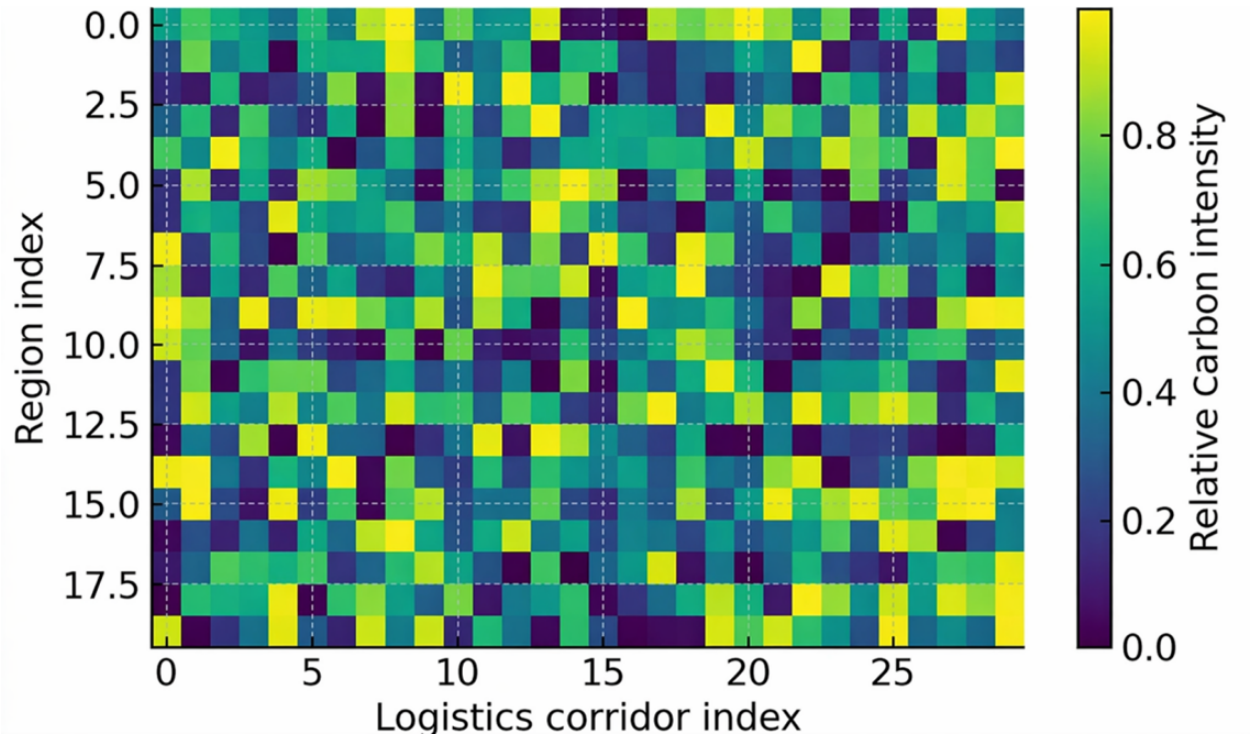

Figure 1. Carbon emissions distribution heatmap

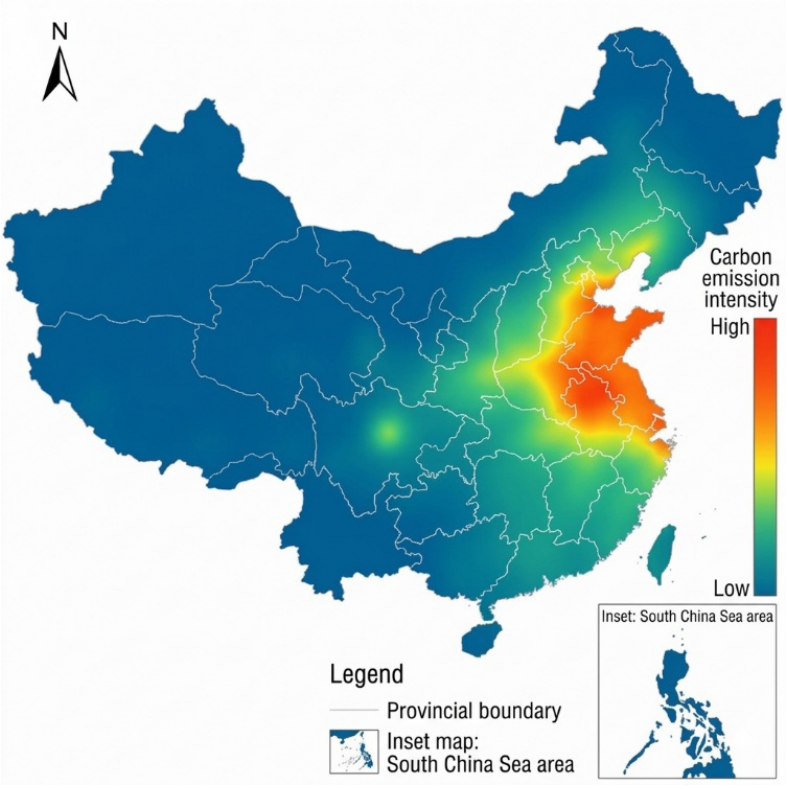

Figure 2. Spatial distribution of logistics carbon emission intensity across China

produced by the prediction model and aggregated to the corresponding region/agent level. Network externalities were incorporated via a node importance multiplier, so that for key nodes identified by centrality (c_i), policy intensity may be scaled as $s_i = s(1+\lambda c_i)$ and $p_i = p(1+\lambda c_i)$ to represent targeted regulation on supernodes.

3.2.1. Payoff structure and parameterization

Let $k \in E, S$ denote the enterprise and supplier. Their baseline emissions (no abatement) are E_k^0, and emissions under abatement are E_k^A, with emission reduction $\triangle E_k = E_k^0 - E_k^A$ estimated from the data-driven carbon accounting pipeline in Section 3.1. Abatement incurs a convex cost $C_k\left(\triangle E_k\right) = \frac{1}{2} k_k \left(\triangle E_k\right)^2$, where k_k captures marginal abatement difficulty. Market demand/reputation effects are captured by a net benefit for adopting low-carbon practices, while non-abatement may incur a reputational loss under strict regulation. This quadratic convex cost specification, which implies increasing marginal abatement costs as emission reductions deepen, is widely adopted in climate economy and policy modeling to reflect this.[85,86] Robustness to the abatement cost functional form was assessed in Section 3.2.4 (linear and piecewise linear costs); the subsidy–penalty threshold regions and convergence directions were qualitatively unchanged.

Policy tools included an emission reduction subsidy and an excess emission penalty. For agent $k \in E, S$, the subsidy under the regulation regime g is proportional to realized emission reduction (**Equation 3**):

$$Sub_k^g = s_g \cdot \Delta E_k, \text{ with } s_g \geq 0 \tag{3}$$

For emissions exceeding an allocated quota $\overline{\mathrm{E}}_k$, the penalty was imposed on the positive part of excess emissions (**Equation 4**):

$$Pen_k^g = p_g \cdot \max(0, E_k^g - \overline{E}_k), \text{with } p_g \geq 0 \tag{4}$$

Lenient regulation was modeled by weaker intensities $(s_L, p_L) = (\eta_s s_R, \eta_p p_R)$ with $0 \leq \eta_s, \eta_p < 1$, whereas strict regulation used s_R, p_R. For numerical convenience and cross-scenario comparability, this study normalized subsidy and penalty coefficients as $S = s_R / s_0$ and $P = p_R / p_0$, where s_0 and p_0 are baseline scaling constants (e.g., policy-relevant unit rates).

Given regulation regime $g \in R, L$, the enterprise and supplier payoffs are defined as follows. Let $I(\cdot)$ be an indicator function and let $E_E = E_E^1$, if A_E is chosen (otherwise E_E^0); similarly for E_S. Coordination/network externalities were captured by complementarity terms $\phi_E \cdot \Delta E_S \cdot I(A_S)$ and $\phi_S \cdot \Delta E_E \cdot I(A_E)$, representing, for example, upstream low-carbon adoption improving downstream carbon performance and market access. Then, we obtain **Equations 5** and **6**:

$$\begin{aligned} \pi_E(g, A_E) = {} & \pi_E^0 + B_E \cdot I(A_E) \\ & - C_E(\Delta E_E) \cdot I(A_E) \\ & + \phi_E \cdot \Delta E_S \cdot I(A_S) + Sub_E^g \\ & - Pen_E^g - L_E \cdot I(N_E) \cdot I(g = R) \end{aligned} \tag{5}$$

$$\begin{aligned} \pi_S(g, A_S) = {} & \pi_S^0 + B_S \cdot I(A_S) \\ & - C_S(\Delta E_S) \cdot I(A_S) \\ & + \phi_S \cdot \Delta E_E \cdot I(A_E) + Sub_S^g \\ & - Pen_S^g - L_S \cdot I(N_S) \cdot I(g = R) \end{aligned} \tag{6}$$

Government payoff (net social welfare) was specified as: $W_G(g) = W_0 - d \cdot (E_E + E_S) - (Sub_E^g + Sub_S^g) + (Pen_E^g + Pen_S^g) - C_r eg \cdot I(g = R)$, where $d > 0$ is the unit of social damage of emissions and C_{reg} is the administrative cost of strict regulation.

3.2.2. Replicator dynamics

Let π_G^R and π_G^L denote the expected payoffs of strategies *R* and *L* for the government, and similarly let π_E^A and π_E^N, and π_S^A and π_S^N, denote expected payoffs for the enterprise and supplier. Expectations are based on the mixed strategies and the payoff matrix in Table 2. The tripartite replicator dynamics system is given as **Equations 7–9**:

$$dx / dt = x(1-x) \cdot (U_G^R - U_G^L) \tag{7}$$

$$dy / dt = y(1-y) \cdot (U_E^{A_E} - U_E^{N_E}) \tag{8}$$

$$dz / dt = z(1-z) \cdot (U_S^{A_S} - U_S^{N_S}) \tag{9}$$

This system yields eight pure strategy equilibria $(x, y, z) \in 0,1^3$ and (potentially) interior mixed equilibria when payoff differences are zero. In the empirical section, this study computed response surfaces over normalized policy intensities (S, P) and heterogeneous initial conditions to reflect the low initial penetration of low-carbon strategies in logistics practice.

For the simulation design, (*S*, *P*) were evaluated on a uniform grid *S*, *P* ∈ {0.0, 0.1, …, 1.0}. For each grid point, the replicator dynamics were run for *T* = 5,000 steps (Δ*t* = 0.01) and declared convergence when max{|dx/dt|,|dy/

Table 2. Payoff matrix of the tripartite evolutionary game

Enterprise/ supplier	Government: Strict regulation (*R*)		Government: Lenient regulation (*L*)	
	Supplier: Proactive (A_S)	Supplier: Passive (N_S)	Supplier: Proactive (A_S)	Supplier: Passive (N_S)
Enterprise: Proactive (A_E)	$\pi_{E0}+B_E-C_E(\Delta E_E)+\phi_E\cdot\Delta E_S+Sub_E^R-Pen_E^R$ $\pi_{S0}+B_S-C_S(\Delta E_S)+\phi_S\cdot\Delta E_E+Sub_S^R-Pen_S^R$ $W_0-d\cdot(E_E+E_S)-(Sub_E^R+Sub_S^R)$ $+(Pen_E^R+Pen_S^R)-C_{reg}$	$\pi_{E0}+B_E-C_E(\Delta E_E)+Sub_E^R-Pen_E^R$ $\pi_{S0}+\phi_S\cdot\Delta E_E-Pen_S^R-L_S$ $W_0-d\cdot(E_E+E_S)-Sub_E^R$ $+(Pen_E^R+Pen_S^R)-C_{reg}$	$\pi_{E0}+B_E-C_E(\Delta E_E)+\phi_E\cdot\Delta E_S+Sub_E^L-Pen_E^L$ $\pi_{S0}+B_S-C_S(\Delta E_S)+\phi_S\cdot\Delta E_E$ $+Sub_S^L-Pen_S^L$ $W_0-d\cdot(E_E+E_S)-(Sub_E^L+Sub_S^L)+$ $(Pen_E^L+Pen_S^L)$	$\pi_{E0}+B_E-C_E(\Delta E_E)+Sub_E^L-Pen_E^L$ $\pi_{S0}+\phi_S\cdot\Delta E_E-Pen_S^L$ $W_0-d\cdot(E_E+E_S)-Sub_E^L$ $+(Pen_E^L+Pen_S^L)$
Enterprise: Passive (N_E)	$\pi_{E0}+\phi_E\cdot\Delta E_S-Pen_E^R-L_E$ $\pi_{S0}+B_S-C_S(\Delta E_S)+Sub_S^R-Pen_S^R$ $W_0-d\cdot(E_E+E_S)-Sub_S^R$ $+(Pen_E^R+Pen_S^R)-C_{reg}$	$\pi_{E0}-Pen_E^R-L_E$ $\pi_{S0}-Pen_S^R-L_S$ $W_0-d\cdot(E_E+E_S)$ $+(Pen_E^R+Pen_S^R)-C_{reg}$	$\pi_{E0}+\phi_E\cdot\Delta E_S-Pen_E^L$ $\pi_{S0}+B_S-C_S(\Delta E_S)+Sub_S^L-Pen_S^L$ $Sub_S^L+(Pen_E^L+Pen_S^L)$	$\pi_{E0}-Pen_E^L$ $\pi_{S0}-Pen_S^L$ $W_0-d\cdot(E_E+E_S)$ $+(Pen_E^L+Pen_S^L)$

Note: A_E / A_S denote proactive abatement; N_E / N_S denote passive/non-abatement. $E_k^{\,0}$ and $E_k^{\,1}$ are baseline and abatement emissions ($k\in\{E,S\}$), with $\Delta E_k=E_k^{\,0}-E_k^{\,1}>0\cdot\ Sub_k^g=s_g\cdot\Delta E_k$ and $Pen_k^g=p_g\cdot\max\left(0,E_k-\bar{E}_k\right)$ for $g\in R\ L$. Under strict regulation *R*, non-abatement incurs reputational loss L_E, L_S, and the government pays the administrative cost C_{reg}. Under lenient regulation *L*, $(s_L,p_L)=(\eta_s s_R,\eta_p p_R)$ with $0\le\eta_s,\eta_p<1$. Network externalities enter through $\varphi_E\cdot\Delta E_S$ and $\varphi_S\cdot\Delta E_E$; for key nodes with centrality c_i, effective policy intensities may be scaled as ($s_g\cdot[1+\lambda c_i]$, $p_g\cdot[1+\lambda c_i]$). For passive strategy *N*, set $\Delta E_k=0$ (thus $Sub_k^g=0$) and use $E_k^g=E_k$ in Pen_k^g; for proactive strategy *A*, use $E_k^g=E_k$ in Pen_k^g.

dt|,|dz/dt|} < 1e−6 for 200 consecutive steps. Response surfaces were reported under heterogeneous initial conditions reflecting low initial penetration: $x0\in\{0.1,0.3\}$, $y0\in\{0.05,0.2\}$, $z0\in\{0.05,0.2\}$. Sensitivity analyses over these settings are summarized in Supplementary 2.

3.2.3. Equilibria and formal stability analysis

Let $F\left(x,y,z\right)$ denote the replicator dynamics vector field. The Jacobian matrix $J\left(x,y,z\right)=DF\left(x,y,z\right)$ was used for local stability analysis. As each component has the form $\Delta(u,\cdot)$, all cross-partials vanish at the pure equilibria $(x^*,y^*,z^*)\in\left\{0,1\right\}^3$; hence, the Jacobian becomes diagonal at each vertex (x^*,y^*,z^*). The eigenvalues are therefore:

$$\lambda_x=(1-2x^*)\cdot(U_G^R-U_G^L)\,|_{(x^*,y^*,z^*)} \tag{10}$$

$$\Lambda_y=(1-2y^*)\cdot(U_E^{A_E}-U_E^{N_E})\,|_{(x^*,y^*,z^*)} \tag{11}$$

$$\Lambda_z=(1-2z^*)\cdot(U_S^{A_S}-U_S^{N_S})\,|_{(x^*,y^*,z^*)} \tag{12}$$

A pure equilibrium is locally asymptotically stable (evolutionarily stable strategy (ESS) in the local sense) if and only if all three eigenvalues are negative. Table 3 summarizes the stability conditions for the eight pure equilibria, enabling analytical identification of subsidy/penalty thresholds that separate passive from proactive regimes.

Here, $\Delta_G=U_G^R-U_G^L$, $\Delta_E=U_E^{A_E}-U_E^{N_E}$, and $\Delta_S=U_S^{A_S}-U_S^{N_S}$, evaluated at the corresponding equilibrium. In particular, at the proactive equilibrium $E8=(1,1,1)$, the enterprise's net incentive to abate under strict regulation simplifies to: $\Delta_E=(B_E+L_E)-C_E(\Delta E_E)+s_R\cdot\Delta E_E+p_R\cdot[(E_E^0-\bar{E}_E)^+-(E_E^1-\bar{E}_E)^+]$, and analogously for the supplier: $\Delta_S=(B_S+L_S)-C_S(\Delta E_S)+s_R\cdot\Delta E_S+p_R\cdot[(E_S^0-\bar{E}_S)^+-(E_S^1-\bar{E}_S)^+]$. Therefore,

threshold lines in the (S,P) plane can be obtained by setting $\Delta_E = 0$ and $\Delta_S = 0$ after substituting $s_R = S \cdot s_0$ and $p_R = P \cdot p_0$. These analytical thresholds were cross-validated by the response surface simulations reported in the empirical section.

Table 3. Eigenvalue-based local stability conditions for the eight pure equilibria

Equilibrium	(x^*, y^*, z^*)	Local stability (all eigenvalues < 0)
E1	(0,0,0)	Δ_G < 0, Δ_E < 0, Δ_S < 0
E2	(1,0,0)	Δ_G > 0, Δ_E < 0, Δ_S < 0
E3	(0,1,0)	Δ_G < 0, Δ_E > 0, Δ_S < 0
E4	(0,0,1)	$\Delta_G < 0, \Delta_E < 0, \Delta_S > 0$
E5	(1,1,0)	$\Delta_G > 0, \Delta_E > 0, \Delta_S < 0$
E6	(1,0,1)	$\Delta_G > 0, \Delta_E < 0, \Delta_S > 0$
E7	(0,1,1)	$\Delta_G < 0, \Delta_E > 0, \Delta_S > 0$
E8	(1,1,1)	$\Delta_G > 0, \Delta_E > 0, \Delta_S > 0$

Specifically, the evolution of corporate and governmental strategies can be modeled using a composite network framework that allows for mutual influence through information networks between enterprises across different regions or types. Simulation calculations of system evolution under varying initial conditions and parameter values yielded response surface plots (Figure 3). Response surface analysis visualized the impact of parameter changes on equilibrium stability, thereby verifying whether high subsidies combined with moderate penalties can gradually steer enterprises toward emission reduction strategies. Simulations were conducted using MATLAB (R2023b) to ensure convergence and test the robustness of different parameter combinations.

Additionally, radar charts or heatmaps can be used to visualize enterprise or supply chain performance metrics when comparing the efficiency of various strategy combinations. Figure 3 presents a radar chart comparing the comprehensive efficiency of different strategies across multidimensional indicators, including economic, environmental, and technological benefits. Retailers tend to increase subsidies rather than share costs to incentivize manufacturers' emissions reductions. In contrast, cooperative models achieved Pareto optimality across the entire chain through profit sharing. Radar charts enable clear comparisons of strategy performance across dimensions, helping decision-makers balance costs with environmental outcomes.

At the policy tool level, the government provided (targeted) emission reduction subsidies and imposed excess emission penalties. The operational definitions of the subsidy and penalty functions are given in **Equations 3** and **4** in Section 3.2.1, and the normalized intensities (S, P) were used as the key policy levers in the subsequent response surface simulations.

3.2.4. Sensitivity to abatement cost functional form

In the baseline specification, abatement cost was modeled as quadratic and convex, implying increasing marginal abatement costs as emission reductions deepen. In an alternative specification with linear costs, the quadratic cost was replaced with a linear function $C_k^l in(\Delta E_k) = c_k \cdot \Delta E_k$. To ensure comparability, c_k was calibrated so that $C_k^{lin}(\Delta E_k^{ref})$ equals the baseline quadratic cost at a reference reduction level ΔE_k^{ref} (e.g., the median reduction implied by the data-driven accounting pipeline). For Alternative B (piecewise-linear convex cost), this study considered a two-segment convex approximation: $C_k^p w(\Delta E_k) = c1_k \cdot \Delta E_k$ for $0 \le \Delta E_k \le \Delta \bar{E}_k$, and $C_k^p w(\Delta E_k) = c1_k \cdot \Delta \bar{E}_k + c2_k \cdot (\Delta E_k - \Delta \bar{E}_k)$ for $\Delta E_k > \Delta \bar{E}_k$, with $c2_k > c1_k$. Parameters $(c1_k, c2_k, \Delta \bar{E}_k)$ were calibrated to match the baseline quadratic cost at $\Delta E_k = \Delta \bar{E}_k$ and at a reference reduction level ΔE_k^{ref}, preserving increasing marginal abatement difficulty while relaxing the quadratic assumption.

For each cost specification {quadratic, linear, piecewise linear}, the replicator dynamics simulations were rerun on the same (S, P) grid and the same integration settings as in Section 3.2.2 (T = 5,000, Δt = 0.01, convergence tolerance 1e−6) under the same heterogeneous initial conditions. For each (S, P) point, this study recorded the long-run convergence direction of (y, z) and compared the induced threshold curve $P_{crit}(S)$ separating the high-adoption region ($y \to 1$, $z \to 1$) from the low-adoption region when a stable equilibrium was reached.

The qualitative conclusions did not depend on the quadratic functional form. Across linear and piecewise linear costs, (i) the S–P phase diagram retained the same

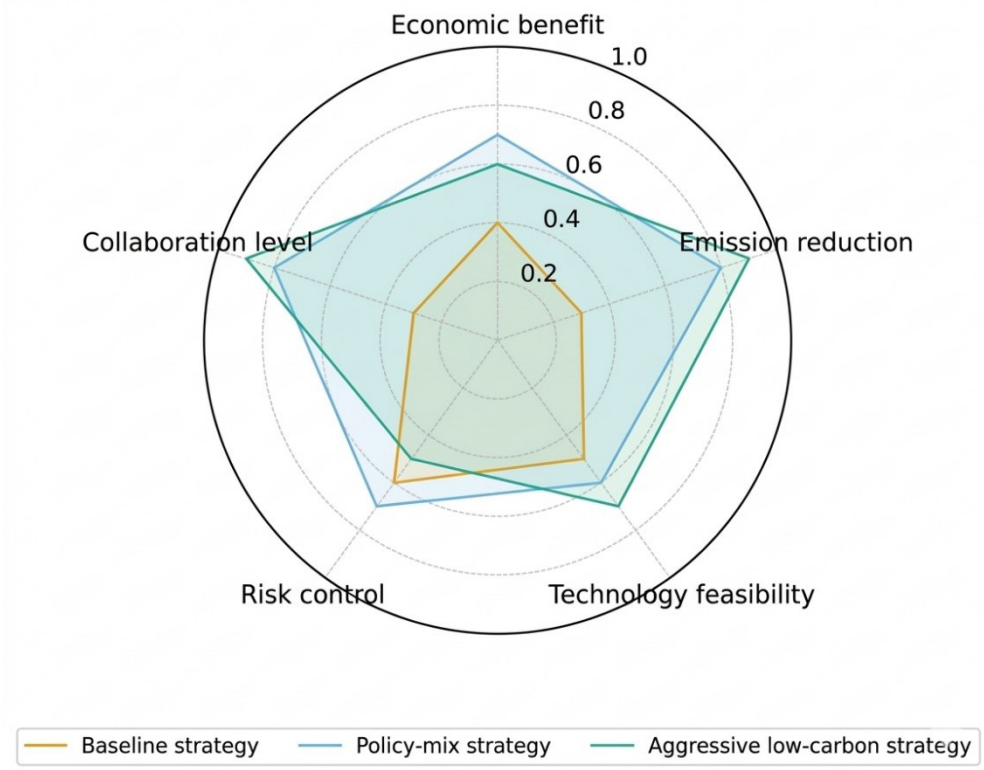

Figure 3. Comparative radar chart evaluation of three logistics transition strategies across five dimensions. All scores were normalized to a 0–1 scale, where higher values indicate better performance on the corresponding criterion.

monotone structure (higher S expands the high-adoption region; higher P contracts it), and (ii) convergence directions and the identity of stable equilibria remained unchanged. Quantitatively, the critical boundary $P_{crit}(S)$ shifted by at most one grid step (≤0.1 in normalized units) across all tested initial conditions.

3.3. Statistical analysis

Model-comparison significance was assessed using the Nadeau–Bengio corrected paired t-test based on fold-level error differences from time-series cross-validation. Rank concordance across centrality measures was evaluated using Spearman correlation coefficients, and top-k overlap was assessed using the Jaccard index. All statistical analyses were conducted using Python (version 3.12) and MATLAB (R2023b). Statistical significance was set at $p < 0.05$. Community-structure analysis was further conducted on the logistics–carbon emission linkage network using the Louvain community-detection algorithm. The weighted-directed network was partitioned into communities by maximizing network modularity (Q), and the average clustering coefficient (C) was reported to characterize the degree of local agglomeration among connected nodes. This procedure was used to identify stable regional clusters, distinguish intra-community concentration from inter-community bridge connections, and support the interpretation of the spatially clustered carbon-flow patterns observed in the empirical analysis.

4. Results and discussion

4.1. Data, regions, and sample composition

This empirical study, conducted within the methodological framework, utilized three types of data.:

(i) Macro statistics from sources such as the National Statistical Yearbook and industry annual reports were used to construct annual freight scale and structure for each province, with a focus on key logistics nodes, such as the Beijing–Tianjin–Hebei region, the Yangtze River Delta, and the Pearl River Delta.

(ii) Logistics enterprise survey data, including TMS orders, routes, transport distances, vehicle types and energy sources, load factors, and delivery timeliness.

(iii) Vehicle travel data for calibrating unit activity emission factors and operational conditions at the micro level. The data timeframe primarily covers 2018–2023, with exogenous variables such as holidays, weather, and

oil prices integrated for model interpretation and scenario analysis.

To ensure consistency, this study standardized metric units, identified outliers, imputed missing values, and applied lag expansion and normalization to key time-series variables.

Public databases and direct URLs used for the secondary aggregated statistics (accessed on 26 Dec 2025) are listed below.

(i) National Bureau of Statistics of China, China Statistical Yearbook (2018–2023):

- 2018: https://www.stats.gov.cn/sj/ndsj/2018/indexeh.htm
- 2019: https://www.stats.gov.cn/sj/ndsj/2019/indexeh.htm
- 2020: https://www.stats.gov.cn/sj/ndsj/2020/indexeh.htm
- 2021: https://www.stats.gov.cn/sj/ndsj/2021/indexeh.htm
- 2022: https://www.stats.gov.cn/sj/ndsj/2022/indexeh.htm
- 2023: https://www.stats.gov.cn/sj/ndsj/2023/indexeh.htm

(ii) National data annual transport and freight indicators (including "Basic Conditions of Transport" tables):

- https://data.stats.gov.cn/easyquery.htm?cn=C01
- https://data.stats.gov.cn/english/tablequery.htm?code=AC0T

(iii) Ministry of Transport of the People's Republic of China, Statistics Data portal:

- https://www.mot.gov.cn/tongjishuju/

(iv) China Federation of Logistics and Purchasing, official statistical releases and reports (public reposts for accessibility):

- https://en.ndrc.gov.cn/netcoo/achievements/202111/t20211125_1305237.html
- https://en.ndrc.gov.cn/news/pressreleases/202207/t20220728_1332801.html
- https://en.ndrc.gov.cn/netcoo/achievements/202302/t20230223_1349822.html
- https://www.chinadaily.com.cn/a/202204/16/WS625cc95fa310fd2b29e578af.html

Micro-level operational data (TMS order flows, routes, OBD/GPS) were collected from participating logistics enterprises' internal systems and are not publicly accessible via an online database.

To address data transparency and representativeness, Table 4 summarizes the time coverage, geographic scope, and sample composition of each data stream (macro statistics, enterprise TMS order flows, and OBD/GPS travel records), including missing data rates after cleaning. Variable definitions and data sources are provided in Table S1. For confidentiality reasons, raw micro-level records are not released; however, the reported counts and coverage allow readers to assess external validity and potential selection bias. For transparency and interpretability, Table 5 reports descriptive statistics in original units after cleaning and covers all feature families used in the baseline model and in the subsequent leave-one-feature-group-out (LOFO) ablation and SHAP analyses. For model fitting and evaluation, continuous features were standardized (z-scores) within each training/validation split.

COVID-19 disruptions (2020–2022) were explicitly handled in both modeling and interpretation. This study included a pandemic regime indicator (and interactions with fuel price and congestion proxies) and reports model performance separately for pre-COVID (2018–2019), COVID (2020–2022), and post-COVID (2023) periods. In addition, the out-of-time split (Section 4.2) keeps the 2023 test set fully held out to avoid leakage and evaluate post-shock generalization.

For encoded categorical variables, the reported mean and standard deviation summarize the empirical distribution of observed codes and are provided for completeness; these values should not be interpreted as ordinal magnitudes.

4.2. Prediction models and evaluation framework

The modeling strategy adopted a "divide-and-conquer + ensemble" approach: first, training models grouped by business lines and energy types; then aggregating them via stacking generalization for global forecasting. Continuous features were standardized (z-score) within the training folds used for model fitting; Table 5 presents descriptive statistics in original units after cleaning to facilitate interpretation.

4.2.1. Out-of-time back testing and time-series validation protocol

The prediction target was the carbon emission intensity y, measured in kg CO_2 per ton km (computed from activity data and calibrated using the emission factors described in Section 3.1). To ensure leakage-free evaluation on temporal data, this study adopted an out-of-time split: trained on 2018–2021, validated on 2022 (for hyperparameter selection), and tested on 2023 (for final reporting). Within the training window, hyperparameters were selected using an expanding window time-series cross-validation

Table 4. Sample composition, coverage, and key variables

Data stream	Unit of observation	Time coverage	Geographic coverage	Sample size (after cleaning)	Key variables (examples)	Missing rate after cleaning (key fields)
Macro statistics (NBS/MoT/CFLP)	Province-year / city-year	2018–2023	China (31 provinces; key hubs)	186 province-year observations	Freight volume, turnover, modal split, energy mix, price indices	Not applicable (published aggregates)
Enterprise TMS order flows	Order/shipment	2018–2023 (monthly/daily)	Prefecture-level cities involved in sampled routes	1.2 M cleaned records	OD pair, distance, payload, load factor, service type, cold chain flag	Table S3
Vehicle OBD/GPS/telematics	Trip/trajectory segment	2018–2023	Sampled fleets & routes	4.8 M segment observations	Speed, acceleration, idling, road grade proxy, fuel/energy type	Table S3
Merged modeling dataset	Order-trip matched record	2018–2023	Same as above	Derived from matched TMS and OBD/GPS streams (subset of above)	Target *y*: emission intensity (kg carbon dioxide per ton km); features: load factor, average vehicle speed, acceleration fluctuation, gradient, congestion index, vehicle type, energy/fuel type, route/business type, weather condition, fuel price, holidays/seasonality, and trip distance	Table S3

Abbreviations: CFLP: China Federation of Logistics and Purchasing; GPS: Global positioning system; MoT: Ministry of Transport; NBS: National Bureau of Statistics; OBD: On-board diagnostics; OD: Origin–destination; TMS: Transport management system.

scheme with $K = 5$ folds, a one-month forecast horizon (H = 1), and a one-month gap (G = 1) between the end of the training fold and the start of the validation fold to prevent look-ahead bias. Table 6 reports the final selected hyperparameters (best validation RMSE over the search grid), and Table 7 reports performance on the held-out 2023 test set.

4.2.2. Robustness checks for temporal stability and shock periods

To address robustness concerns, this study conducted three complementary out-of-sample checks designed to prevent temporal leakage: (i) out-of-time split, all feature engineering procedures (Table S4) used information available up to the forecast origin; (ii) rolling-window back testing using a fixed-length 36-month training window, a 6-month validation window, and a 1-month test step, rolling forward month by month to obtain a distribution of errors across time; and (iii) COVID-19 structural-break check by re-estimating models for a pandemic regime (Jan 2020–Dec 2021) and reporting pre-COVID vs. COVID vs. post-COVID performances. These robustness checks and related supplementary analyses are summarized in Table S5, including the rolling-window design, the COVID-19 structural-break diagnostics, and a corrected significance-testing setup.

To ensure reproducibility and comparability, hyperparameter tuning and selection for the tree ensemble LightGBM model, the SVR model, and the sparse linear baseline Lasso model were conducted within a unified data preprocessing and validation framework, as shown

Table 5. Descriptive statistics of the full feature families used in model fitting, LOFO ablation, and SHAP interpretation

Feature category	Variable name	Unit / Encoding	Mean	Standard deviation	Range	SHAP/LOFO relevance
Target variable	Carbon emission intensity	kg CO_2/ (ton km)	0.094	0.013	0.066, 0.138	Model prediction target
Operational factors	Congestion index	Index (0–10)	1.42	0.38	0.73, 3.00	Key driver for speed/acceleration
	Average vehicle speed	km/h	58.6	12.4	29.5, 84.9	U-shaped effect on emissions
	Acceleration fluctuation	m/s^2	0.45	0.18	0.23, 0.96	Captures driving behavior
	Gradient (slope)	Degrees (°)	1.85	1.12	0.00, 5.68	High impact on energy consumption
Loading and structural	Load factor	% (0–100)	78.4	12.5	39.4, 94.0	High importance in SHAP ranking
	Vehicle type	0: Light, 1: Medium, 2: Heavy	1.34	0.76	0, 2	Categorical; structural factor
	Energy/fuel type	0: Diesel, 1: Gas, 2: Electric	0.42	0.54	0, 2	Directly affects the emission factor
	Route/business type	0: Trunk, 1: Branch, 2: Urban	0.82	0.65	0, 2	Explains scenario heterogeneity
Exogenous shocks	Weather condition	0: Clear, 1: Rain/ Snow	1.28	0.45	1.00, 2.47	Significant environmental shock
	Fuel price	CNY/L	7.82	0.64	6.57, 9.82	Economic driver for cost/load optimization
	Holidays/seasonality	Binary (0 or 1)	0.15	0.36	0, 1	Captures transport demand peaks
Network and logistics	Trip distance	km	425.6	185.3	140.2, 966.7	Core operational metric

Abbreviations: LOFO: Leave-one-feature-group-out; SHAP: Shapley additive explanation.

in Table 6. Data preprocessing employed a pipeline of "numeric feature standardization and categorical feature one-hot encoding." Validation utilized time-series cross-validation and layer-wise holdout, with weighted MAPE as the primary evaluation metric based on business volume. RMSE and MAPE are also reported for comparative analysis.

The tree ensemble LightGBM model was selected as the preferred approach due to the evident nonlinear and interactive effects between carbon emission intensity and factors such as load factor, speed deviation, congestion, and road gradient. A smaller learning rate combined with a moderate number of base learners helped balance fitting capability and stability in time-series scenarios; shallow tree depth suppressed overfitting while enhancing interpretability. Subsampling was employed to enhance model randomness and improve generalization performance.

Table 6. Final hyperparameters selected by grid search under expanding window time-series cross-validation (validation year: 2022)

Model	GBDT (proxy for LightGBM)	SVR (RBF)	Lasso
n_estimators	300	—	—
learning_rate	0.05	—	—
max_depth	3	—	—
subsample	0.9	—	—
C	—	5	—
gamma	—	scale	—
epsilon	—	0.02	—
alpha	—	—	0.001
max_iter	—	—	5,000
normalize	StandardScaler in pipeline	StandardScaler in pipeline	StandardScaler in pipeline

Abbreviations: GBDT: Gradient-boosted decision trees; GBM: Gradient boosting machine; RBF: Radial basis function; SVR: Support vector regression.

Table 7. Forecast error comparison on the held-out out-of-time test set (2023)

Model	RMSE	MAPE	Weighted MAPE
GBDT	0.00554	0.04340	0.04113
Lasso	0.00949	0.09533	0.06871
SVR	0.01258	0.12498	0.09677

Note: RMSE is reported in kg CO_2 per ton km.
Abbreviations: GBDT: Gradient-boosted decision trees; MAPE: Mean absolute percentage error; RMSE: Root mean square error; SVR: Support vector regression.

To provide a strong, yet structurally simple, nonlinear comparison, this study trained a radial basis function kernel SVR model. Here, *C* controls the trade-off between kernel range and error penalty; gamma influences the curvature of high-dimensional mappings; and epsilon determines the ε-insensitivity loss bandwidth. SVR results served as robustness and significance benchmarks against tree models. As an interpretability baseline, this study configured Lasso-regularized linear regression. Lasso mitigated multicollinearity through coefficient sparsification and provided approximate "main effect" direction estimates, facilitating sensitivity analysis and contribution decomposition.

All three models underwent hyperparameter search via time-series cross-validation, with search ranges guided by empirical intervals and prior knowledge. To ensure reproducibility while accounting for stochasticity, the cross-validation splits were fixed, and for stochastic learners such as LightGBM/GBDT, training was repeated across 10 random seeds (0–9). Deterministic learners (SVR, Lasso) yielded identical results across seeds. Tables 6–8 report the median performance across seeds, while Table S6 summarizes the time-series validation settings, the random seed design, and the selected hyperparameters used to assess model stability and reproducibility.

Among the evaluation metrics shown in Table 7, GBDT achieved the lowest RMSE, while SVR and Lasso recorded higher values. Regarding MAPE and weighted MAPE metrics, GBDT performed best under both overall and freight volume-weighted criteria, with weighted MAPE highlighting the model's advantage on "heavy-load long-distance" samples. Compared to SVR and Lasso, GBDT

demonstrated significantly superior performance in RMSE and weighted MAPE, indicating that tree ensembles better capture the nonlinear combined effects of load factor, vehicle speed, and congestion.

As shown in Table 8, the tree ensemble model achieved lower RMSE and weighted MAPE than SVR and Lasso on the held-out 2023 test set. To avoid inflated significance due to temporal dependence, a Nadeau–Bengio-corrected paired *t*-test was conducted using fold-level error differences from time-series cross-validation as the effective sample size. The corrected *p*-values confirm that LightGBM/GBDT significantly outperformed baselines while respecting the independence assumptions.

4.2.3. Feature-group ablation and stability of key thresholds

A LOFO ablation was performed to test whether the results are overly dependent on any single feature family. Specifically, we retrained the preferred GBDT/LightGBM model after removing one feature group at a time (load-related, speed-related, congestion, weather, fuel price, and route type) and re-evaluated performance on the 2023 out-of-time test set. Table 9 reports the RMSE, MAPE, and weighted MAPE, along with the corresponding deltas (Δ) relative to the full model, and verifies whether the key threshold findings remained stable (the load factor threshold of 0.7–0.8 and the U-shaped speed effect). The descriptive statistics for all feature families entering the LOFO ablation and SHAP interpretation are reported in Table 5. Ablation confirms that the threshold findings were not driven by a single feature family.

Load factor exhibited a monotonically decreasing trend with diminishing returns in Figure 4A. Marginal emission reductions peaked in the 0.7–0.8 range, while the curve flattened beyond 0.85. Therefore, a target load factor threshold should be established to prioritize merging low-load orders. Average vehicle speed exhibited a U-shaped pattern. Both low-speed congestion and high-speed rapid acceleration/deceleration increased per-unit emissions, with an optimal window around 45–60 km/h in Figure 4B. Route planning should prioritize congestion avoidance and steady-state speed, with operational key performance indicators set for critical corridors.

Marginal effects varied across routes and vehicle types.

Table 8. Corrected the significance test of forecast errors

Comparison	*t*-statistics	*p*-value (corrected)	Mean difference (RMSE)
SVR vs. GBDT	14.32	1.69e−07	0.00704
Lasso vs. GBDT	12.26	6.43e−07	0.00395

Note: Nadeau–Bengio-corrected paired *t*-test; fold-level differences.
Abbreviations: GBDT: Gradient-boosted decision trees; RMSE: Root mean square error; SVR: Support vector regression.

Table 9. Feature-group ablation and stability of key thresholds

Removed feature group	RMSE (Δ)	MAPE (Δ)	Load threshold (0.7–0.8) stability
None (full model)	0.00554 (0)	0.0434 (0)	Yes
Load-related	+0.00421	+12.5%	Yes
Speed-related	+0.00278	+8.2%	Yes
Congestion index	+0.00155	+4.1%	Yes
Weather factors	+0.00042	+0.9%	Yes
Fuel price	+0.00028	+0.3%	Yes

Abbreviations: MAPE: Mean absolute percentage error; RMSE: Root mean square error.

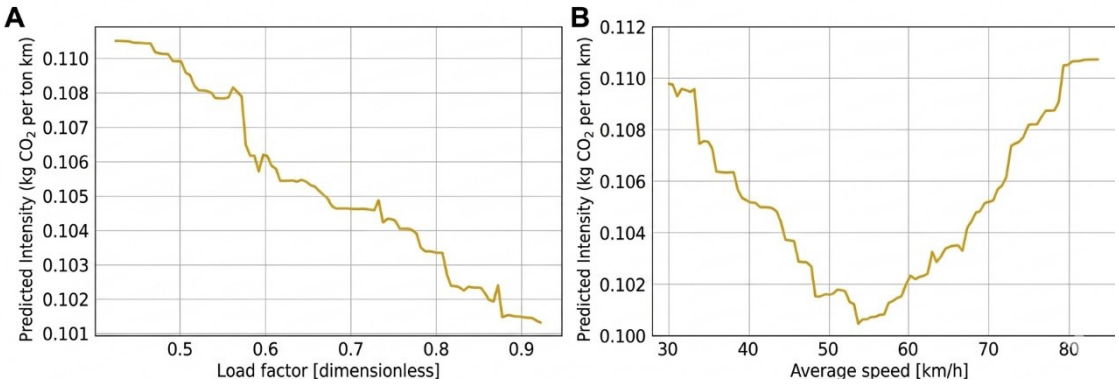

Figure 4. Partial dependence plots. (A) Load factor. (B) Average vehicle speed.

Curves appeared flatter in the cold chain and urban short-haul samples, indicating that temperature control and stop-start operations partially offset load-dilution effects in Figure 5. Management should establish thresholds by business line to avoid one-size-fits-all approaches.

In summary, the tree ensemble model trained on multi-source data significantly outperformed the baseline model in RMSE and weighted MAPE, with paired tests confirming statistically significant differences. Partial dependence plot analysis revealed diminishing returns thresholds for load factors and a U-shaped relationship with vehicle speed, consistent with existing research showing that increasing load and steady-state speed significantly reduce emission intensity. Individual conditional expectation (ICE) further confirms pronounced heterogeneity in marginal effects across cold chain and urban scenarios, echoing industry reports that highlight these scenario differences. Consequently, this study translates threshold discoveries into operational rules and demonstrates, through game simulations, that "high subsidies + moderate penalties" drive corporate strategies toward a low-carbon equilibrium, achieving an integrated, closed-loop of prediction–explanation–incentivization.

4.3. Overall trends and driving factors

Based on the fitted results of road freight volume and structure from 2018 to 2023, national logistics carbon emissions reached a phased peak around 2021. Subsequently, emissions declined slightly alongside optimization of the transport capacity structure and adjustments to the transport distance structure, exhibiting

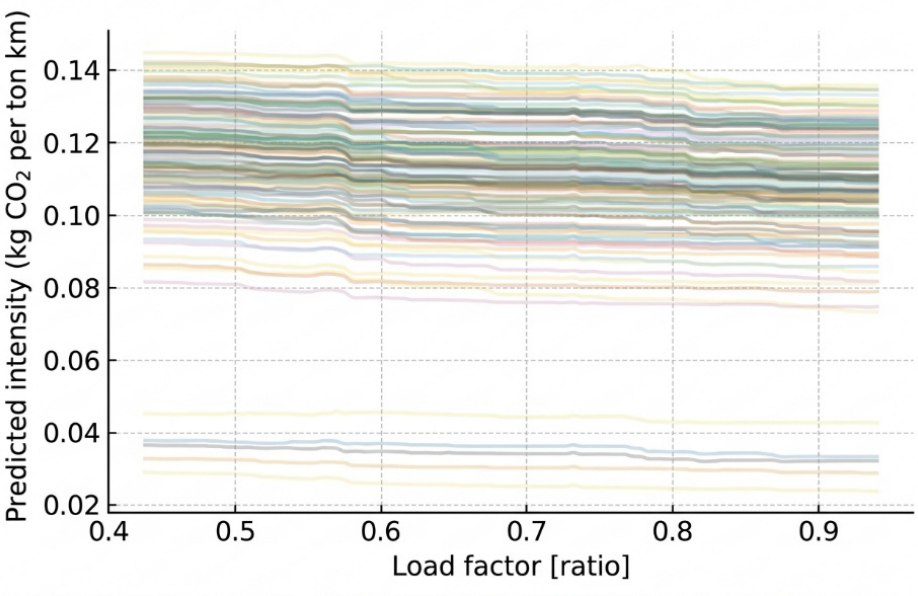

Figure 5. Individual load capacity curve

an overall "high-level plateauing" trend. This finding is consistent with recent literature suggesting that, although the post-pandemic period may create opportunities for transport decarbonization, absolute reductions in transport emissions remain unlikely without stronger low-carbon policies and structural adjustments.[87] Factor decomposition revealed three primary drivers of emission intensity: (i) operational conditions such as congestion/average vehicle speed, acceleration fluctuations, and gradient; (ii) loading and structural factors including load factor, vehicle type and energy source, and business attributes like cold chain/express logistics; and (iii) exogenous shocks like holidays, weather, and fuel prices. In the SHAP global ranking, congestion index, load factor, and energy type ranked highest. Partial dependence curves showed that marginal emission reductions were most significant at load factors of 0.7–0.8, with diminishing returns thereafter. Average speed exhibited a U-shaped relationship—both excessively slow and excessively fast speeds increase emissions per unit of freight volume. These findings provide a basis for threshold-based operational management.

4.4. Carbon emission network topology: Identifying key nodes and corridors

A weighted-directed network was constructed using prefecture-level cities/national-level new areas as nodes, based on OD flows, transport distances, and unit activity emission factors from enterprise TMS orders. Key regions covered logistics hubs, including Beijing–Tianjin–Hebei, the Yangtze River Delta, the Pearl River Delta, Chengdu–Chongqing, and the middle Yangtze River.

4.4.1. Hub cities: Coexistence of high connectivity and high intensity

Weighted degree centrality revealed that national emissions were dominated by a few "super nodes" (Figure 6), with Shanghai, Wuhan, Guangzhou, Shenzhen, Zhengzhou, Nanjing, Hangzhou, Chongqing, Hefei, and Beijing in the top 10. The top 10% of nodes accounted for approximately 58% of the network's weighted degree; the top 5% accounted for most of the cross-regional trunk emission flows. These cities simultaneously possess multiple attributes—ports, airports, rail marshalling hubs, and large distribution parks—explaining their combined characteristics of "connectivity breadth + intensity." Consistent with the spatial hotspots in Figures 1 and 2, these high-centrality nodes highly overlap with the high-value belt along the eastern coastal-central corridor. A small number of "super nodes" bear the bulk of carbon flow aggregation and distribution functions within the network, making them critical targets for improving overall emission efficiency and governance effectiveness. Implementing fleet electrification, load factor threshold management, and multimodal transport integration at these hubs can achieve a "point-to-belt" carbon reduction spillover effect. The bootstrap confidence interval and the null-model test for this concentration statistic are reported in Table S5.

To validate the concentration estimate, the uncertainty of the "top 10% share" was quantified using nonparametric bootstrapping. Specifically, the OD edges were resampled with replacement (B = 2,000 replicates), the weighted degree for each replicate was recomputed, and a 95% bootstrap confidence interval was obtained for the top 10% contribution share. To assess whether the observed concentration exceeds what would be expected by chance, the results were compared against a degree-preserving null model (a configuration model with the same in/out-degree sequence, repeated R = 1,000 times), and the null distribution and a one-sided permutation p-value were reported. The concentration validation design and summary reporting are documented in Table S5.

In addition to weighted degree and betweenness, PageRank, eigenvector centrality, Katz centrality, and collective influence were computed on the same weighted-directed network. Rank concordance was assessed using Spearman correlations and top k overlap. Additionally, substantial overlap and strong positive rank correlations were observed across these centrality families; the centrality-concordance framework is documented in Table S7. This indicates that the identification of key emission nodes is not an artifact of a single centrality definition.

4.4.2. Bridge nodes: Corridor "checkpoints" significantly impact cross-regional carbon flows

Intermediary centrality rankings revealed that cities like Zhengzhou, Wuhan, Hefei, Nanchang, Xi'an, and Changsha—situated at the intersections of north–south and east–west corridors—handle substantial "transit" functions for shortest paths: approximately 32% of shortest path sets traverse at least one bridging node. Simulations revealed that "modifying" the top 1% edges by intermediary centrality—while maintaining network connectivity—could reduce total emissions by 8–11% in a single step. Directly "removing" these edges would redirect emissions to suboptimal channels, increasing average path length by 6–9%, suggesting that "substitution over blocking" is preferable.

4.4.3. Community structure: Pronounced endogenous agglomerations within industrial belts and metropolitan areas

Louvain clustering identified 4–5 stable communities:

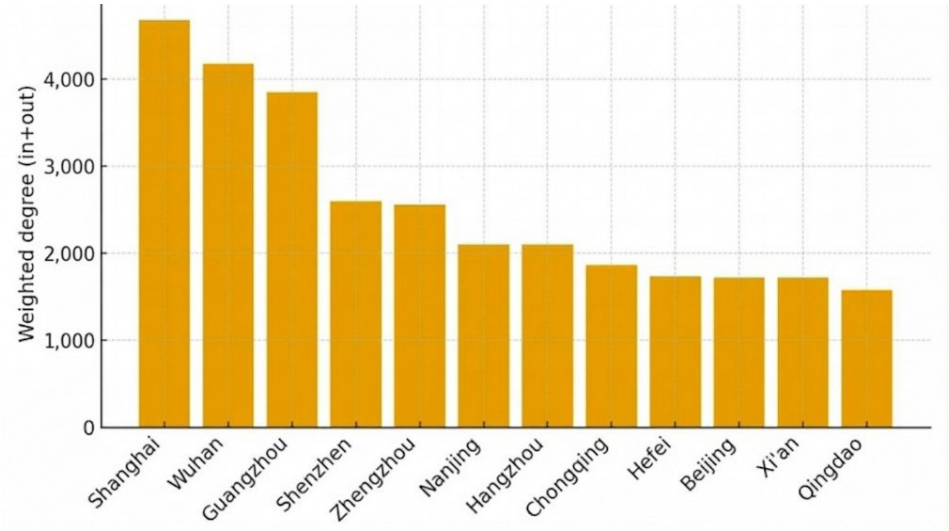

Figure 6. Weighted rank the top 12 hub cities

Bohai Rim, Yangtze River Delta, Pearl River Delta–South China Coast, Chengdu–Chongqing–Western Corridor, and Middle Yangtze River. Network modularity ($Q \approx 0.46$) and average clustering coefficient ($C \approx 0.38$) revealed pronounced regional clustering. Intra-community "short-radius, high-frequency" distribution/supply reinforced clustering, while inter-community connections relied relatively on a few bridging nodes. Figure 7 reveals pronounced regional clustering aligning with industrial belts and metropolitan spatial organization. Within communities, collaborative measures like park-based mutual replenishment, shared delivery, nighttime off-peak scheduling, and standardized turnover should reduce per-unit emissions for the "last 100 kilometers." Cross-community connections relied on a few bridging nodes, necessitating differentiated corridor governance.

4.4.4. Edge distribution and backbone: Heavy-tail characteristics coexist with "long trunk lines–short branch lines"

Edge weights exhibited a typical heavy-tail distribution, with the top 5% of edges contributing approximately 41% of weighted emission flows. The backbone network adopted a "long trunk lines + radial branch lines" structure, with trunk lines primarily following coastal and Yangtze River corridors, while branch lines further distribute emissions to metropolitan areas and industrial parks. The steepness of the curve in Figure 8 indicates a pronounced heavy tail in the network—a small number of high-weight pathways carry the majority of carbon flows. This allows defining a "backbone network," in which the top 20% or top 10% of edges are prioritized for mitigation efforts.

4.5. Multi-agent evolutionary game model

The simulation employed a three-party game model involving the government, a typical logistics enterprise, and suppliers. Initially, all parties adopted passive emission reduction strategies under lax government regulation. Multiple simulations were conducted by adjusting subsidy parameters (S) and penalty parameters (P) to track system evolution. Results indicate that when the government provided higher subsidies and moderately increased penalties, logistics enterprises and suppliers gradually evolved toward active emission reduction strategies, ultimately achieving a low-carbon stable equilibrium. Otherwise, enterprises tend to maintain passive emission reduction, leading the system into a high-emission state. Figure 9 illustrates the response surface of this process, showing that as S increases and P is moderately raised, the overall emission level at the evolutionary equilibrium point decreases significantly. This finding aligns with the existing literature: high incentives, coupled with moderate regulation, promote the diffusion of low-carbon technologies.

4.5.1. Simulation parameterization and reproducibility

To make the response surface simulations in Figure 9 reproducible, this study reports the assumed baseline values and ranges for subsidy intensity S, penalty intensity P, initial strategy shares, baseline emissions, and emission reduction cost parameters in Table 10. When parameters are calibrated from empirical evidence, ML-derived marginal effects are mapped to payoff components (e.g., the load factor threshold of 0.7–0.8 and the speed window

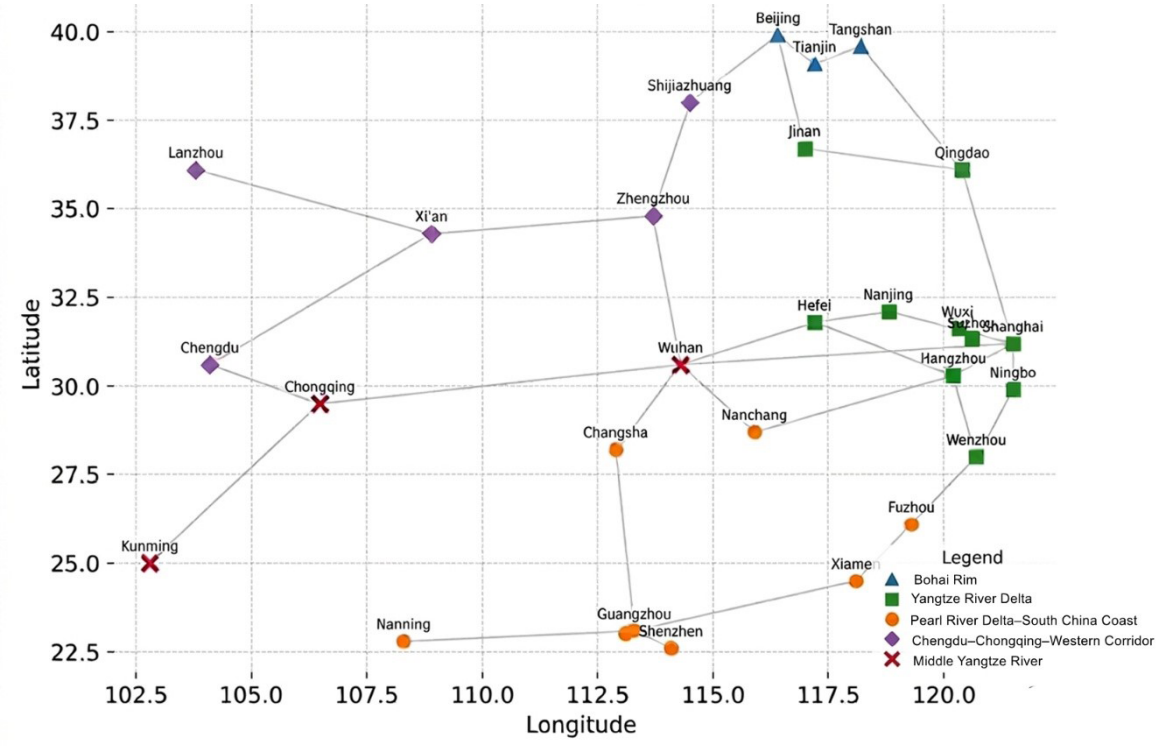

Figure 7. Community structure diagram. Node shapes distinguish communities.

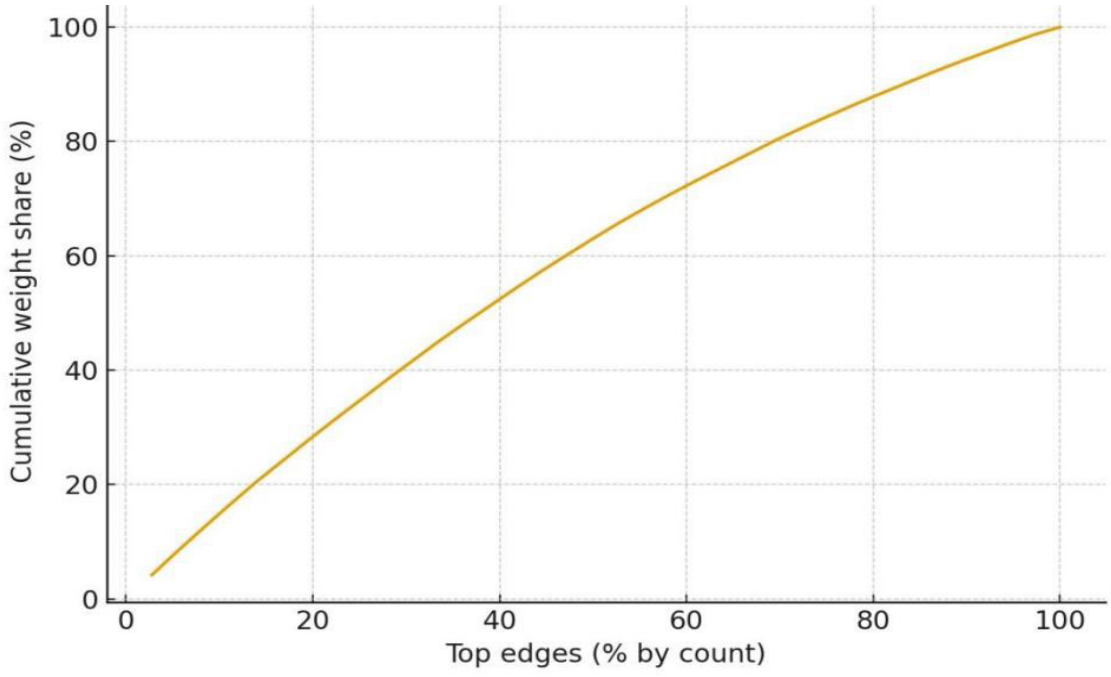

Figure 8. Edge weight cumulative proportion

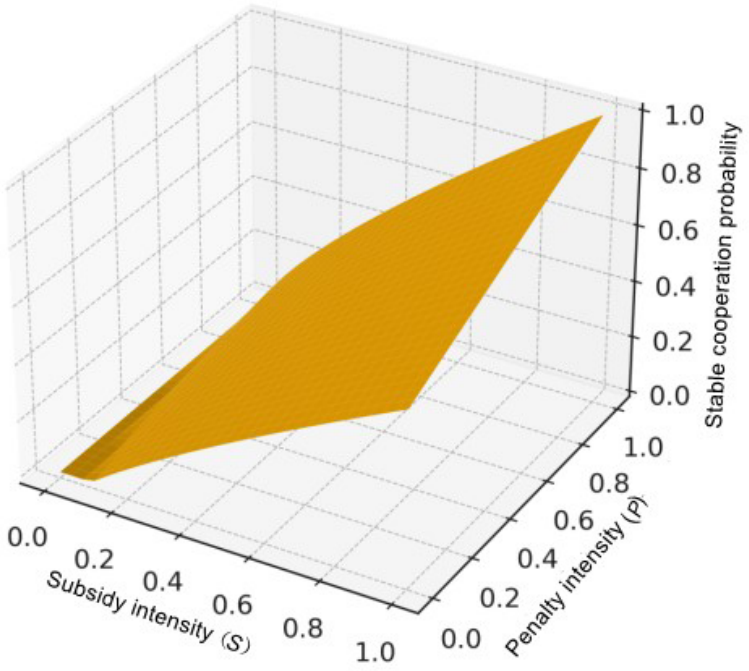

Figure 9. Response surface of government incentives

of 45–60 km/h) by translating operational improvements into expected reductions in emission intensity (Δy) and cost savings. These quantified effects are reflected in the utilities of both the enterprise and the supplier as measurable benefits.

4.5.2. Simulation settings and convergence diagnostics

Replicator dynamics were simulated for T=5,000 iterations with step size Δt = 0.01. Convergence was declared when $\max\{|x\_\{t + 1\} - x\_t|, |y\_\{t + 1\} - y\_t|, |z\_\{t + 1\} - z\_t|\} < \varepsilon$ = 1e−6 for m=200 consecutive steps. To account for parameter uncertainty, Monte Carlo simulations (M=500 runs) were conducted by sampling key parameters (η, c, and baseline emissions) within the sensitivity ranges in Table 10, and mean trajectories and 95% simulation intervals for adoption shares were generated. These diagnostics ensured that the reported S-shaped adoption dynamics are not sensitive to initial conditions or single-point parameter choices.

Model simulations also revealed the strategic interactions among multiple stakeholders. As subsidies were gradually phased in, the frequency of corporate carbon reduction strategies increased in an S-shaped manner as shown in Figure 9. Furthermore, the radar comparison of different strategy combinations in Figure 3 demonstrated that cooperative emission reductions not only lowered overall emissions but also balanced costs and market benefits. Investments in optimizing transportation networks and procuring new-energy vehicles may yield long-term returns. Overall, the combined evidence from big-data forecasting and policy simulation provides intuitive support for decision-making.

4.6. Policy recommendations

Based on empirical evidence (Sections 4.1–4.5) and multi-agent evolutionary game simulations (Figure 9), this study proposes an implementation-oriented policy toolbox for accelerating low-carbon transitions in green logistics supply chains. The recommendations are designed to be measurable (MRV-ready) and to map directly onto the model levers S (subsidy intensity) and P (penalty intensity). The implementation-oriented policy toolbox derived from the empirical findings and simulation results is summarized in Table 11.

4.6.1. Establish a standardized measurement, reporting, verification, and data-sharing infrastructure for logistics carbon accounting

In practice, regulators can adopt ISO 14083/ISO 14067 and the Greenhouse Gas Protocol to define system boundaries, activity data fields (vehicle type, fuel/energy, load factor, distance, route), and verification procedures. A minimum reporting dataset at the trip or shipment level (after de-identification) should be required for major carriers

Table 10. Evolutionary game simulation parameters, baseline values, and ranges

Parameter	Symbol	Baseline value	Range (sensitivity)	Calibration/source
Subsidy intensity (normalized)	S	0.60	$S \in [0,1]$	Policy scenario design; normalized from the unit subsidy coefficient in **Equation 3**
Penalty intensity (normalized)	P	0.45	$P \in [0,1]$	Policy scenario design; normalized from unit penalty coefficient in **Equation 4**
Initial government strategy share	$x0$	0.30	[0,1]	Set to reflect baseline policy strictness
Initial enterprise low-carbon share	$y0$	0.10	[0,1]	Scenario design to reflect low initial adoption; sensitivity tested
Initial supplier compliance share	$z0$	0.10	[0,1]	Scenario design to reflect low initial compliance; sensitivity tested
Baseline emission intensity	y_base	1.00 (unit-normalized)	[0.5, 1.5] (normalized)	Normalized baseline from emission model outputs; robustness over scaling range
Emission reduction effectiveness	η	0.20	[0.05, 0.50]	Scenario-based effectiveness; calibrated within plausible ranges; sensitivity tested
Abatement cost parameter	c	0.30	[0.10, 0.80]	Scenario-based cost parameter; calibrated within plausible ranges; sensitivity tested

and key suppliers, enabling reproducible carbon footprint estimates and third-party audits.

4.6.2. Implement centrality-guided targeting to allocate limited policy resources

Using the weighted-logistics-carbon emission linkage network constructed in this study, governments can compute multiple centrality metrics (e.g., PageRank/Katz/eigenvector or collective influence) to identify high-leverage nodes (top k provinces/cities/hubs/enterprises). Regulatory inspections, green-corridor pilots, and subsidy budgets should be prioritized for these nodes, as marginal improvements propagate through the network and yield larger system-level reductions.

4.6.3. Calibrate subsidies and penalties using the response-surface results to avoid ineffective or excessive interventions

The simulations indicate a threshold region in which the system transitions from a high-emission equilibrium to a stable low-carbon equilibrium. Policymakers should (i) set the subsidy at or above a minimum level S^* to overcome initial adoption barriers, and (ii) choose a penalty within the empirically identified effective interval (P_min, P_max) documented in Figure 9 and summarized in Table S5, which deters free-riding without triggering excessive compliance costs. Both subsidy and penalty can be updated dynamically based on observed adoption rates and measured emission intensity, with explicit budget

constraints and sunset rules for mature technologies. In our normalized policy-intensity scale (0–1) and grid simulations (step 0.1), the transition region was approximately $S^* \approx 0.6$, and the effective moderate penalty window was $P \in [0.3, 0.6]$.

4.6.4. Promote contract-based incentives across the supply chain to align enterprise and supplier behavior

Logistics enterprises can incorporate carbon performance into supplier selection and contracts (e.g., carbon-indexed procurement, shared savings for verified reductions, and penalties for non-compliance). Suppliers can be incentivized to provide low-carbon materials and services/services and to provide transparent data, thereby reducing information asymmetry and improving the effectiveness of policy instruments.

4.6.5. Operationalize the transition through a phased roadmap with measurable key performance indicators

(i) Phase I (pilot): Implement MRV standards and centrality-based targeting in a subset of high-centrality nodes.
(ii) Phase II (scale-up): Expand successful instruments

Table 11. Implementation-oriented policy toolkit for low-carbon governance in green logistics supply chains

Policy instrument	Lead actor	Targeting/trigger rule	MRV indicator (KPI)	Ref.
MRV & reporting	Govt./regulator	Mandatory for major carriers & key suppliers; de-identified trip-level reporting	Verified emission intensity (kg CO_2/ton km), data completeness	Sections 4.1–4.2
Centrality-based targeting	Govt./city authority	Prioritize top k nodes by centrality (PageRank/Katz/collective influence) for pilots & inspections	Concentration metrics; top k contribution share; network stability	Section 4.4
Subsidy design (S)	Govt./finance	Set $S \geq S^*$ for early-stage adoption; sunset as adoption stabilizes (approx.: $S^* \approx 0.6$ on normalized 0–1 scale)	Adoption rate; marginal abatement per subsidy unit	Figure 9
Penalty design (P)	Govt./regulator	Choose P within (P_min, P_max) documented in Figure 9 and summarized in Table S5; escalate only when repeated non-compliance (approx.: $P \in [0.3, 0.6]$ on normalized 0–1 scale)	Violation rate; verified emissions; compliance cost proxy	Figure 9
Supply chain contracting	Enterprise (lead firm)	Carbon-indexed contracts; shared savings; supplier disclosure requirement	Supplier carbon score; contract compliance; Scope 3 intensity	Section 4.5

Abbreviations: KPI: Key performance indicator; MRV: Measurement, reporting, and verification.

across regions and business lines (trunk, urban, cold chain), and integrate with carbon trading/green finance.

(iii) Phase III (continuous improvement): Monitor key performance indicators (emission intensity, adoption rate, network concentration of emissions) and iterate subsidy/penalty settings based on periodic evaluation.

5. Conclusion

This study addresses challenges in carbon footprint measurement in green logistics supply chains by integrating big data-enabled carbon tracking with network analytics and a multi-agent evolutionary game model. Empirically, this study constructed an logistics-carbon emission linkage network and demonstrated that emissions are structurally concentrated in a small set of high-centrality nodes, which provided a practical basis for targeted interventions. Methodologically, the proposed framework connected predictive analytics and explainability to mechanism design, enabling policymakers to translate data evidence into calibrated incentives and penalties.

Overall, the results suggest that centrality-guided targeting can amplify system-level abatement, while the response surface analysis highlights a threshold region for effective policy design: subsidies must reach a minimum level to initiate adoption, and penalties should be set within an effective interval to deter free-riding without inducing excessive compliance burdens. Together, these findings offer an actionable pathway to coordinate governments, logistics enterprises, and suppliers toward a stable low-carbon equilibrium. The study's limitations and future recommendations include:

(i) Data availability and confidentiality: Part of the operational dataset is proprietary, which limits full public release. Future work can provide a de-identified benchmark dataset and detailed data dictionaries to improve reproducibility.

(ii) Structural breaks: The 2018–2023 period included major events (e.g., COVID-19) that may affect behavioral and network dynamics; additional stress-testing and scenario-based validation are warranted.

(iii) Network construction and metric sensitivity: Results may vary with alternative edge definitions and centrality measures; further robustness checks with null models and multi-layer networks will strengthen external validity.

(iv) Behavioral heterogeneity: The evolutionary game abstracts from firm heterogeneity and learning across heterogeneous fleets and contracts; extending the model to heterogeneous agents and calibrating parameters with micro-level surveys or transaction data is a promising direction.

Acknowledgments

None.

Funding

None.

Conflict of interest

The authors declare they have no competing interests.

Author contributions

Conceptualization: Lin Sun
Formal analysis: Lin Sun
Investigation: Lin Sun
Methodology: Lin Sun
Project administration: Jun Zeng
Supervision: Jun Zeng
Writing–original draft: Lin Sun
Writing–review & editing: All authors

Availability of data

The data that support the findings of this study are available from the corresponding author upon reasonable request.

References

1. World Economic Forum. Intelligent Transport, Greener Future: AI as a Catalyst to Decarbonize Global Logistics. White paper. January 2025.

2. National Development and Reform Commission. Working Guidance for Carbon Dioxide Peaking and Carbon Neutrality in Full and Faithful Implementation of the New Development Philosophy. Published October 24, 2021. Accessed April 5, 2026.

3. International Energy Agency. China. Accessed April 5, 2026.

4. China Academy of Transportation Sciences. Report on Sustainable Transport in China. Beijing: Ministry of Transport of the People's Republic of China; 2021. Available from: https://xxgk.mot.gov.cn/jigou/gjhzs/202112/P020211214343055452953.pdf [Last accessed on March 17, 2026].

5. Huang Y, Wang K, Zhang T, Pang C. Green supply chain coordination with greenhouse gases emissions management: a game-theoretic approach. *J Clean Prod*. 2016;112:2004-2014.

   doi: 10.1016/j.jclepro.2015.05.137

6. Tian J, Jia F, Chen L, Xing X. The impact of ISSB's Scope 3 GHG emissions validation on US manufacturers' stock valuations: analyzing the role of supplier complexity. *Transp*

Res Part E Logist Transp Rev. 2025;193:103850.

doi: 10.1016/j.tre.2024.103850

7. Pan S, Ivanov D, Chutani A, *et al*. New normal, new norms: towards sustainable and resilient global logistics and supply chain management. *Transp Res Part E Logist Transp Rev*. 2025;201:104276.

doi: 10.1016/j.tre.2025.104276

8. Liew M, Cao J. Accounting for carbon emissions through green supply chain management: a systematic literature review. *Bus Strategy Environ*. 2025;34(7):8281-8304.

doi: 10.1002/bse.70021

9. Alves MYF, Vieira LM, Partyka RB. Suppliers' GHG mitigation strategies (Scope 3): the case of a steelmaking company. *J Manuf Technol Manag*. 2024;35(2):383-402.

doi: 10.1108/JMTM-05-2023-0162

10. Ellram LM, Tate WL. Impact pathways: a call for impactful research in supply chain GHG emissions reduction. *Int J Oper Prod Manag*. 2025;45(1):236-245.

doi: 10.1108/IJOPM-07-2023-0574

11. Çapar İ, Rump CM, Sawaya W, *et al*. Green supply chain evolution: a multimodal logistics strategy for capping carbon emissions. *Transp Res Part E Logist Transp Rev*. 2025;202:104250.

doi: 10.1016/j.tre.2025.104250

12. Belhadi A, Venkatesh M, Kamble S, Abedin MZ. Data-driven digital transformation for supply chain carbon neutrality: insights from cross-sector supply chain. *Int J Prod Econ*. 2024;270:109178.

doi: 10.1016/j.ijpe.2024.109178

13. Hua J, Wang K, Lin J, Qian Y. Carbon tax vs. carbon cap-and-trade: implementation of carbon border tax in cross-regional production. *Int J Prod Econ*. 2024;274:109317.

doi: 10.1016/j.ijpe.2024.109317

14. Chen Y, Feng Y, Lai KH, Zhu Q. Value of blockchain for scope 3 carbon disclosure: the moderating role of data processing technologies. *Int J Prod Econ*. 2025;279:109445.

doi: 10.1016/j.ijpe.2024.109445

15. Zhang Y, Huang M, Wu Y, *et al*. Green fourth-party logistics network design under carbon cap-and-trade policy. *Int J Prod Econ*. 2025;282:109540.

doi: 10.1016/j.ijpe.2025.109540

16. Bui TD, Nguyen TTV, Wu KJ, Lim MK, Tseng ML. Green manufacturing performance improvement under uncertainties: an interrelationship hierarchical model. *Int J Prod Econ*. 2024;268:109117.

doi: 10.1016/j.ijpe.2023.109117

17. Saurav A, Yadav V, Shekhar C. An inventory optimization model for reliable and sustainable supply chains under trade credit and carbon constraints. *Supply Chain Anal*. 2025;11:100132.

doi: 10.1016/j.sca.2025.100132

18. Zhou X, Zhu Q, Xu L, *et al*. The effect of carbon tariffs and the associated coping strategies: a global supply chain perspective. *Omega*. 2024;122:102960.

doi: 10.1016/j.omega.2023.102960

19. Parupalli A. Sustainable supply chain practices for scope 3 emissions mitigation: an integrated modeling and optimization perspective. *Int J Emerg Res Eng Technol*. 2025;6(4):146-156.

doi: 10.63282/3050-922X.IJERET-V6I4P118

20. Harju A, Karttunen E, Hallikas J. Understanding the systemic sources of uncertainty for the management of greenhouse gas emissions in supply chains. *Int J Oper Prod Manag*. 2025;45(11):1884-1909.

doi: 10.1108/IJOPM-04-2024-0349

21. Mashud AHM, Chakrabortty RK, Hussain OK, Choi TM. Reducing emissions from production and distribution in three-echelon supply chains. *Int J Prod Econ*. 2024;271:109181.

doi: 10.1016/j.ijpe.2024.109181

22. Cheng J, Liao L, Lu S, *et al*. Effective MILP and matheuristic for multi-echelon green supply chain operations and financing considering carbon emission reduction investment. *J Clean Prod*. 2025;493:144816.

doi: 10.1016/j.jclepro.2025.144816

23. Kallionpää E, Viri R, Tiikkaja H, *et al*. The data logistics cannot deliver: emissions reporting of logistics in Finland. *Liikenne-vuosikirja*. 2025;8:9-58.

doi: 10.58956/liikenne.178422

24. Lu X, Xu X, Sun Y. Enhancing resilience in supply chains through resource orchestration and AI assimilation: an empirical exploration. *Transp Res Part E Logist Transp Rev*. 2025;195:103980.

doi: 10.1016/j.tre.2025.103980

25. Shmuel A, Glickman O, Lazebnik T. A comprehensive benchmark of machine and deep learning models on structured data for regression and classification. *Neurocomputing*. 2025;655:131337.

doi: 10.1016/j.neucom.2025.131337

26. Jiang J, Sheng D. Multi-period regional low-carbon logistics network planning with uncertain demand. *Energy*. 2025;331:137068.

doi: 10.1016/j.energy.2025.137068

27. Hasani Goodarzi A, Jabbarzadeh A, Fahimnia B, Paquet M. Evaluating the sustainability and resilience of an intermodal

transport network leveraging consolidation strategies. *Transp Res Part E Logist Transp Rev*. 2024;188:103616.

doi: 10.1016/j.tre.2024.103616

28. Franco de la Peña MF, Perales Gómez ÁL, Fernández Maimó L. ShaTS: a Shapley-based explainability method for time series artificial intelligence models. *Future Gener Comput Syst*. 2026;176:108178.

doi: 10.1016/j.future.2025.108178

29. Nayebi A, Tipirneni S, Reddy CK, *et al*. WindowSHAP: an efficient framework for explaining time-series classifiers based on Shapley values. *J Biomed Inform*. 2023;144:104438.

doi: 10.1016/j.jbi.2023.104438

30. Li S, Tong Z, Haroon M. Estimation of transport CO_2 emissions using machine learning algorithm. *Transp Res Part D Transp Environ*. 2024;133:104276.

doi: 10.1016/j.trd.2024.104276

31. Li M, Tang Y, Wu K, Cheng H. Autonomous vehicle pollution monitoring: an innovative solution for policy and environmental management. *Transp Res Part D Transp Environ*. 2025;139:104542.

doi: 10.1016/j.trd.2024.104542

32. Zhong W, Zhai D, Xu W, *et al*. Accurate and efficient daily carbon emission forecasting based on improved ARIMA. *Appl Energy*. 2024;376:124232.

doi: 10.1016/j.apenergy.2024.124232

33. Luo H, Wang C, Li C, *et al*. Multi-scale carbon emission characterization and prediction based on land use and interpretable machine learning model: a case study of the Yangtze River Delta Region, China. *Appl Energy*. 2024;360:122819.

doi: 10.1016/j.apenergy.2024.122819

34. Yuan D, Tang L, Yang X, Xu F, Liu K. Explainable machine learning prediction of vehicle CO_2 emissions for sustainable energy and transport. *Energies*. 2025;18(20):5408.

doi: 10.3390/en18205408

35. Guo X, Kou R, He X. Towards carbon neutrality: machine learning analysis of vehicle emissions in Canada. *Sustainability*. 2024;16(23):10526.

doi: 10.3390/su162310526

36. Catret-Ruber P, Garcia-Rodriguez D, Iglesias Fuente DJ, *et al*. An open, reproducible benchmark of daily CO_2 forecasting models with applications to GHG monitoring. *Environ Model Softw*. 2026;196:106781.

doi: 10.1016/j.envsoft.2025.106781

37. Şahin V. Explainable machine learning-based prediction of CO_2 emissions from passenger vessels. *Ocean Eng*. 2025;341(Pt 3):122752.

doi: 10.1016/j.oceaneng.2025.122752

38. Zhang SR, Farooq B. Interpretable and actionable vehicular greenhouse gas emission prediction at road link-level. *Sustain Cities Soc*. 2023;92:104493.

doi: 10.1016/j.scs.2023.104493

39. Qiao Q, Eskandari H, Saadatmand H, Sahraei MA. An interpretable multi-stage forecasting framework for energy consumption and CO_2 emissions for the transportation sector. *Energy*. 2024;286:129499.

doi: 10.1016/j.energy.2023.129499

40. Javanmard ME, Tang Y, Martínez-Hernández JA. Forecasting air transportation demand and its impacts on energy consumption and emission. *Appl Energy*. 2024;364:123031.

doi: 10.1016/j.apenergy.2024.123031

41. An M, Fu Y. Forecasting road freight demand and estimating carbon emissions using ConvLSTM: the Chengdu-Chongqing urban cluster case. *Acad J Comput Inf Sci*. 2025;8(1):71-79.

doi: 10.25236/AJCIS.2025.080110

42. Nam H, Byun J, Nam H. Prediction of greenhouse gas emissions from road freight flow in South Korea for sustainable transportation planning. *Heliyon*. 2025;11(2):e41937.

doi: 10.1016/j.heliyon.2025.e41937

43. Liu C, Chen K, Zhang S, *et al*. Optimizing right-of-way allocation in urban expressway ramp influence areas: placement of autonomous vehicle-dedicated lanes and buffer zones. *IEEE Trans Intell Transp Syst*. 2025;26(12):21684-21696.

doi: 10.1109/TITS.2025.3619819

44. Zhao J, Kou L, Wang H, *et al*. Carbon emission prediction model and analysis in the Yellow River basin based on a machine learning method. *Sustainability*. 2022;14(10):6153.

doi: 10.3390/su14106153

45. Bao Z, Wang C, Innab N, *et al*. Evolutionary game theoretical approach for reducing carbon emissions in a complex supply chain organization. *Manage Decis*. 2024.

doi: 10.1108/MD-10-2023-1962

46. Li J, Gao L, Tu J. Evolutionary game analysis of governments' and enterprises' carbon-emission reduction. *Sustainability*. 2024;16(10):4216.

doi: 10.3390/su16104216

47. Wu X, Shu E, Ye D, *et al*. Study on green packaging diffusion in logistics enterprise clusters based on complex network evolutionary game. *J Clean Prod*. 2025;499:145166.

doi: 10.1016/j.jclepro.2025.145166

48. Zhu L, Zhou R, Li X, Zheng L. Analysis of tripartite evolutionary game for maritime supply chain collaboration considering carbon emission governance. *Front Mar Sci*.

2025;12:1552544.

doi: 10.3389/fmars.2025.1552544

49. Wu R, Zhu L, Jiang M. Research on the evolution game of low-carbon operations in cold chain logistics considering environmental regulations and green credit. *Heliyon*. 2024;10(9):e30559.

doi: 10.1016/j.heliyon.2024.e30559

50. Guo L, Zhang Q, Wu J. An evolutionary game model of manufacturers and consumers' behavior strategies for green technology and government subsidy in supply chain platform. *Comput Ind Eng*. 2024;189:109918.

doi: 10.1016/j.cie.2024.109918

51. Xue J, He Y, Gao P, *et al*. Multi-agent evolutionary game model: corporate low-carbon manufacturing, Chinese government supervision, and public media investigation. *Sustainability*. 2022;14(9):5587.

doi: 10.3390/su14095587

52. Deng S, Zhou D, Wu G, *et al*. Evolutionary game analysis of three parties in logistics platforms and freight transportation companies' behavioral strategies for horizontal collaboration considering vehicle capacity utilization. *Complex Intell Syst*. 2023;9(2):1617-1637.

doi: 10.1007/s40747-022-00873-9

53. Huang Y. Evolutionary game analysis of collaborative strategies in fresh e-commerce and cold chain logistics: the role of incentive mechanisms and supervision policies. *Int Rev Econ Finance*. 2025;104:104773.

doi: 10.1016/j.iref.2025.104773

54. Wang L, Ye Z, Lei T, *et al*. Green and low-carbon strategy of logistics enterprises under "dual carbon": a tripartite evolutionary game simulation. *Systems*. 2025;13(7):590.

doi: 10.3390/systems13070590

55. Sun H, Wang K, Du X. Cooperative emission reduction behaviour of supply chain enterprises under cap-and-trade and government subsidies. *Environ Dev Sustain*. 2025;27(1):2549-2579.

doi: 10.1007/s10668-023-03980-w

56. Zhang C, Xu Y, Zheng Y. Blockchain traceability adoption in low-carbon supply chains: an evolutionary game analysis. *Sustainability*. 2024;16(5):1817.

doi: 10.3390/su16051817

57. Guo W, Meng T, Piao Z, *et al*. Research on the evolutionary game of government and enterprises in carbon emission reduction under multi-market coordinated trading. *Front Sustain Energy Policy*. 2024;3:1456264.

doi: 10.3389/fsuep.2024.1456264

58. Wang Y, Luo H, Zhang X, *et al*. Research on evolutionary game of low-carbon logistics in two-level supply chain under carbon tax policy. *Sustain Futures*. 2024;8:100387.

doi: 10.1016/j.sftr.2024.100387

59. Shen L, Yang Q, Hou Y, Lin J. Research on information sharing incentive mechanism of China's port cold chain logistics enterprises based on blockchain. *Ocean Coast Manag*. 2022;225:106229.

doi: 10.1016/j.ocecoaman.2022.106229

60. Zhang G, Zhang Z. An evolutionary game model of a regional logistics service supply chain complex network in a blockchain environment. *Systems*. 2025;13(1):32.

doi: 10.3390/systems13010032

61. Qian X, Shen L, Wang Y, *et al*. Stability analysis of maritime logistics alliance based on blockchain. *Transp Policy*. 2025;163:219-231.

doi: 10.1016/j.tranpol.2024.12.025

62. Oh S, Kim S, Ryu D. Sequential game of an emissions trading scheme. *Energy Econ*. 2025;150:108824.

doi: 10.1016/j.eneco.2025.108824

63. Duggan JE, Ogland-Hand JD, Middleton RS. Modeling CCS policy support: implications for market performance, net emissions, and welfare. *Appl Energy*. 2025;389:125613.

doi: 10.1016/j.apenergy.2025.125613

64. Cheng L, Yu F, Huang P, *et al*. Game-theoretic evolution in renewable energy systems: advancing sustainable energy management and decision optimization in decentralized power markets. *Renew Sustain Energy Rev*. 2025;217:115776.

doi: 10.1016/j.rser.2025.115776

65. Chen D, Huang Y, Tan N, *et al*. Cross-regional economic impact of carbon emission regulations: a quantitative spatial equilibrium model for China. *Struct Change Econ Dyn*. 2024;69:438-462.

doi: 10.1016/j.strueco.2024.03.001

66. Vakili S, Manias P, Armstrong LM, Turnock S. Technical, economic, and environmental assessment of CO_2 ship transport in carbon capture and storage. *J Environ Manage*. 2025;373:123919.

doi: 10.1016/j.jenvman.2024.123919

67. Ma X, Zhao C, Song C, *et al*. The impact of regional policy implementation on the decoupling of carbon emissions and economic development. *J Environ Manage*. 2024;355:120472.

doi: 10.1016/j.jenvman.2024.120472

68. Qian Y, Zeng J, Hao W, *et al*. Spatiotemporal patterns and drivers of urban traffic carbon emissions in Shaanxi, China. *Land*. 2025;14(7):1355.

doi: 10.3390/land14071355

69. Wei H, Zheng C. Spatial network structure and influencing factors of carbon emission intensity in Guangdong-

Hong Kong-Macao Greater Bay Area. *Front Environ Sci*. 2024;12:1380831.

doi: 10.3389/fenvs.2024.1380831

70. Sui F, Shi X, Ding C. Chinese urban carbon emission correlation network: construction, structural characteristics, and driving factors. *Sustainability*. 2025;17(17):7818.

doi: 10.3390/su17177818

71. Yin C, Zeng L, Fu X, Zhong M. Transition of multimodal transport network under different carbon price scenarios. *Transp Policy*. 2025;164:1-26.

doi: 10.1016/j.tranpol.2025.01.027

72. Wang Y, Yao J. Complex network analysis of carbon emission transfers under global value chains. *Environ Sci Pollut Res Int*. 2022;29(31):47673-47695.

doi: 10.1007/s11356-022-19215-9

73. Shan S, Li Y, Zhang Z, *et al*. Identification of key carbon emission industries and emission reduction control based on complex network of embodied carbon emission transfers: the case of Hei-Ji-Liao, China. *Int J Environ Res Public Health*. 2023;20(3):2603.

doi: 10.3390/ijerph20032603

74. Noferini V, Wood R. Efficient computation of Katz centrality for very dense networks via negative parameter Katz. *J Complex Netw*. 2024;12(5):cnae036.

doi: 10.1093/comnet/cnae036

75. Pei S, Teng X, Shaman J, *et al*. Efficient collective influence maximization in cascading processes with first-order transitions. *Sci Rep*. 2017;7:45240.

doi: 10.1038/srep45240

76. Morone F, Makse HA. Influence maximization in complex networks through optimal percolation. *Nature*. 2015;524(7563):65-68.

doi: 10.1038/nature14604

77. Morone F, Min B, Bo L, *et al*. Collective influence algorithm to find influencers via optimal percolation in massively large social media. *Sci Rep*. 2016;6:30062.

doi: 10.1038/srep30062

78. Liu X, Lu J, Zhou B. The impact of green finance on carbon emission intensity in China: mediating and spatial effects. *Front Environ Sci*. 2025;12:1403246.

doi: 10.3389/fenvs.2024.1403246

79. Wan M, Wei D, Yu C. Low-carbon pilot cities and financialization of listed companies: inhibitory effects and policy analysis. *Finance Res Lett*. 2025;71:106386.

doi: 10.1016/j.frl.2024.106386

80. Zhang SS, Yu X, Sun GQ, *et al*. Locating influential nodes in hypergraphs via fuzzy collective influence. *Commun Nonlinear Sci Numer Simul*. 2025;142:108574.

doi: 10.1016/j.cnsns.2024.108574

81. Zhu C, Su Y, Fan R, *et al*. Research on the optimal incentive and constraint mechanisms for corporate carbon information disclosure considering different market contexts: a network-based evolutionary game analysis. *Energy Econ*. 2025;142:108207.

doi: 10.1016/j.eneco.2025.108207

82. Zhang P, Wang T, Yan J. PageRank centrality and algorithms for weighted, directed networks. *Physica A*. 2022;586:126438.

doi: 10.1016/j.physa.2021.126438

83. Stamos I. Transportation networks in the face of climate change adaptation: a review of centrality measures. *Future Transp*. 2023;3(3):878-900.

doi: 10.3390/futuretransp3030049

84. Agryzkov T, Curado M, Pedroche F, *et al*. Extending the adapted PageRank algorithm centrality to multiplex networks with data using the PageRank two-layer approach. *Symmetry*. 2019;11(2):284.

doi: 10.3390/sym11020284

85. Nordhaus WD. Revisiting the social cost of carbon. *Proc Natl Acad Sci USA*. 2017;114(7):1518-1523.

doi: 10.1073/pnas.1609244114

86. Pizer WA. The optimal choice of climate change policy in the presence of uncertainty. *Resour Energy Econ*. 1999;21(3-4):255-287.

doi: 10.1016/S0928-7655(99)00005-6

87. Li L, Loo BPY. Beyond short-term impact of COVID-19 on transport decarbonization: a scenario analysis of passenger and freight transport by mode in China, 2020-2030. *Energ Sustain Soc*. 2024;14:56.